



Norwegian University of
Science and Technology

Feedforward for Stabilization of an Ammonia Synthesis Reactor

Erik Holter

Master of Science in Engineering Cybernetics

Submission date: June 2010

Supervisor: Morten Hovd, ITK

Problem Description

Feedback control is necessary for stabilization of unstable systems. Feedforward on the other hand, is normally used to improve control performance at high frequencies, beyond the achievable bandwidth for stable closed-loop control.

Recently, it has been showed that feedforward can be used to avoid input constraints which would otherwise cause the system to go unstable.

The aim for the assignment will be to illustrate this for a model of an ammonia synthesis reactor with heat integration. The assignment will be based on an existing MATLAB/Fortran77 model. The project will include:

1. Extensions and modifications of the original model, to include a manipulated variable for control, disturbances and input constraints,
2. design of feedforward and feedback controllers,
3. verification of results using simulation.

Supervisor: Professor Morten Hovd

Assignment given: 11. January 2010

Supervisor: Morten Hovd, ITK

Preface

As a part of the two year MSc program in Engineering Cybernetics- here at Norwegian University of Science and Technology (NTNU)- a compulsory master thesis has to be written during the fourth semester.

I changed assignment between the third and fourth semester, so this master thesis is not based on the student project which was carried out in the third semester.

There are a number of people who should be thanked for helping me in this period.

First, for guiding me through this thesis, I would like to give special thank to my supervisor Professor Morten Hovd, at the Department of Cybernetics, for invaluable input during the semester.

Second, for reading through my thesis, great thanks to Annette Aubert.

Third, I also wish to thank my fellow students Haavard Pershon and Inge Bratbakken for all the helpful discussions. Last, but not least, I wish to thank all my fellow students for making my stay here at NTNU and Trondheim a real pleasure.

Abstract

This thesis illustrates different control structures and tries to demonstrate how feed-forward control can be used in stabilizing an unstable ammonia reactor with heat integration. The demonstration of feedforward is done under very special circumstances. While feedback control is necessary for stabilization of the reactor system, feedforward control can be used to avoid input constraints which would otherwise make the input saturate and thereby make the system unstable.

It turned out that the ammonia reactor was not the best system to apply the feed-forward strategies in question. The main reason is a combination of; the existence of the lower (undesired) steady-state operating point (corresponds to extinction of reaction), positive feedback from the heat exchanger and the manipulated variable range of actuation.

The reason is that there are trade offs between making more of the (cold stream) mass flow go through the heat exchanger and making the cold stream mass flow get mixed with the reactor flow between the beds at the quench points. Letting more mass flow entering the heat exchanger will reduce the heat exchanger efficiency. Lowering the efficiency means that the hot stream mass flow through the heat exchanger can not liberate enough heat to the cold stream mass flow entering the heat exchanger. As a result of this, the reactor inlet temperature will decrease because of the positive feedback from the heat exchanger. Thus, it does not exist a range of actuation where the system can be stabilized when influenced by disturbance.

Contents

Preface	i
Abstract	iii
Abbreviations	ix
List of Figures	xi
1 Introduction	1
1.1 Basis for the Project	1
1.2 Aim of Work	1
1.3 Thesis Outlines	1
2 Mathematical Model of the System	2
2.1 Introduction	2
2.2 Reactor Model	4
2.2.1 Mass and Energy Balance	6
2.2.2 Ammonia Synthesis	7
2.2.3 Modeling of Quench Points	7
2.3 Model of Heat Exchanger	8
2.4 ‘Bypass Valve’	9
2.5 State-space Model	12
3 Control of Reactor	14
3.1 Introduction	14
3.2 Open-loop Simulations	15
3.3 PID-controller	18
3.4 P-controller and the Reactor Inlet Temperature as Measurement	18
3.5 PD-controller and the Reactor Outlet as Measurement	19
4 Feedforward Design	22
4.1 Introduction	22
4.2 Stable Disturbance Model	23

4.3	Unstable Disturbance Model:	
	A "Reference Governor" Approach	24
4.3.1	Hankel -Norm and -Singular Values	26
4.4	H_∞ -control and Feedforward	27
5	Simulation Results	30
5.1	With the Reactor Inlet Temperature as Measurement	30
5.1.1	Unconstrained Input	30
5.1.2	Finding an Unstable Operating Point with RHP-poles Further into the RHP	33
5.2	With the Reactor Outlet Temperature as Measurement	35
5.2.1	Unconstrained Input	36
5.2.2	Constrained Input	37
5.2.3	Feedforward	40
6	Discussion	42
6.1	Reactor Model	42
6.2	Reactor Temperature and Pressure	42
6.3	Extinction and Instability	43
6.4	Control of Reactor	44
6.5	Feedforward	44
6.6	Simulink Model	46
7	Conclusion	48
8	Further Work	50
8.1	Control of Ammonia Reactor	50
8.2	Feedforward	50
Appendix:		
A	Numerical Parameters used in the Simulations	52
B	Numerical Solution of the Model Equations	54
C	MATLAB Files	56
C.1	MATLAB Functions used in each Bed	56
C.1.1	Reaction Rate	58
C.2	State-space Models	58
C.3	Nehari Extension	62
C.4	H_∞ -controller	64

C.5 Miscellaneous Functions	65
Bibliography	69

Abbreviations

Here are some terms and abbreviations used through the thesis.

T_o	reactor outlet temperature
T_i	reactor inlet temperature / heat exchanger outlet temperature
T_{feed}	Fresh feed temperature
\dot{m}_c	cold stream mass flow through heat exchanger
\dot{m}_h	hot stream mass flow through heat exchanger
Q_1	mass flow of fresh feed entering quench 1
Q_2	mass flow of fresh feed entering quench 2
Q_3	mass flow of fresh feed entering quench 3
RHP-	Right half plane
LHP-	Left half plane
IMC	Internal model control
SIMC	Skogestad/Simple IMC
P-controller	Proportional controller
PI-controller	Proportional-Integral- controller
PID-controller	Proportional-Integral-Derivative controller
2-DOF	Two Degrees Of Freedom
MPC	Model Predictive Control
NMPC	Nonlinear Model Predictive Control

List of Figures

2.1	Flowsheet of an ammonia synthesis loop with a fixed bed quench cooling reactor.	3
2.2	Ammonia synthesis reactor	5
2.3	Ammonia synthesis reactor including bypass valve	10
2.4	Simulink blockdiagram of reactor	11
3.1	Nonlinear simulation of a drop in fresh feed temperature (T_{feed}) . . .	16
3.2	Nonlinear simulation of decrease in the reactor pressure	17
4.1	Blockdiagram	23
4.2	Feedforward arrangement for an unstable disturbance transfer function	25
4.3	H_{∞} -controller synthesis for a 2-DOF controller	28
5.1	Nonlinear simulation with proportional control	32
5.2	Nonlinear simulation with (large) decrease in temperature feed	34
5.3	Nonlinear simulation with unconstrained input	36
5.4	Nonlinear simulation with unconstrained input and pressure used as disturbance.	37
5.5	Nonlinear simulation with constrained input	38
5.6	Nonlinear simulation with constrained input and feedforward	41

Chapter 1

Introduction

1.1 Basis for the Project

This MSc thesis is carried out for, and proposed by, Professor Morten Hovd. The assignment is developed as a result of the scientific paper; Feedforward for stabilization, written by Morten Hovd and Robert Bitmead[HB07]. This paper demonstrates how feedforward can assist in stabilizing unstable systems.

The paper points out, that one fundamental limitation for unstable systems is that the range of actuation for the inputs¹ must be sufficiently large to avoid saturation. It is well known that when inputs saturate, the feedback path breaks, and the stability of the system is lost.

Jens Balchen et.al.[JGBF03] explains feedforward in the traditional setup as: "Feedforward is used to improve control performance by generating changes in the input which counteracts the influence disturbance has on the system, such that the response does not effect (or has little effect on) the output of the system".

In the paper written by Morten Hovd and Robert Bitmead, feedforward is used to reduce the magnitude of the plant input moves, and hence avoid the instability due to input constraints.

1.2 Aim of Work

The main goal for this work is to illustrate the latter use of feedforward for an ammonia synthesis². A MATLAB/Simulink model of the ammonia reactor with heat

¹The terms input and manipulated variable are both used in this thesis. When dealing with the reactor particularly, the term manipulated variable is used. The term input is used when the discussion is about system in general.

²A stage in production of fertilizer

integration will be developed. The model will be based on a nonlinear dynamic model developed in FORTRAN77 by former Dr. Ing. student at the Department of Chemical Engineering; John C. Morud. One of the main reasons to base the model development on the work done by Morud, was that Morud had industrial data available, provided by Norsk Hydro ASA. This gives us the opportunity to have a realistic study case. The starting point of Morud's study was an incident in an industrial plant, where the ammonia synthesis reactor became unstable with rapid temperature oscillations. The oscillations generally occurs as a result of a drop in reactor pressure or in temperature.

The goal for this thesis is to prevent the instability by the use of the feedforward strategies proposed by Hovd and Bitmead[HB07]. The assignment will include:

- Extensions and modifications of the original model, making the model in Simulink, to include a manipulated variable for control, disturbances and input constraints,
- design of feedforward and feedback controllers
- verification of results using simulation

1.3 Thesis Outlines

The thesis outlines for the remaining chapters are the following:

Chapter 2 presents the mathematical model consisting of two partial differential equations, based on a mass and an energy balance, as well as the ammonia synthesis and kinetics. The model of the heat exchanger and a linearized state-space model are given at the end of the chapter.

The different control strategies used in the simulations are presented in Chapter 3.

The theory and implementation of the feedforward design is given in Chapter 4.

Chapter 5 shows the simulation results for the different control structures applied.

Discussions are made in Chapter 6.

Conclusions are drawn in Chapter 7.

Proposals for further work is given in Chapter 8.

Chapter 2

Mathematical Model of the System

2.1 Introduction

Ammonia is an important chemical with a wide range of applications. Because of its many uses, ammonia is one of the most highly produced inorganic chemicals. Ammonia is mostly used as a fertilizer and for manufacturing other fertilizers, such as; ammonium- nitrate and sulphate, and urea. Ammonia can also be used for refrigeration processes as freezing agent¹ and in explosives.

The ammonia reactor is the hart of the synthesis plant, but the synthesis plant includes not only the reactor but also other auxiliary equipment. Examples of such equipment is compressors, heat exchangers, boilers and separators. The ammonia synthesis which is the basis of the current work (and in the study of Morud[Mor96]) is shown in Figure 2.1.

¹when the liquid vaporizes, it absorbs a large amount of heat from its surroundings

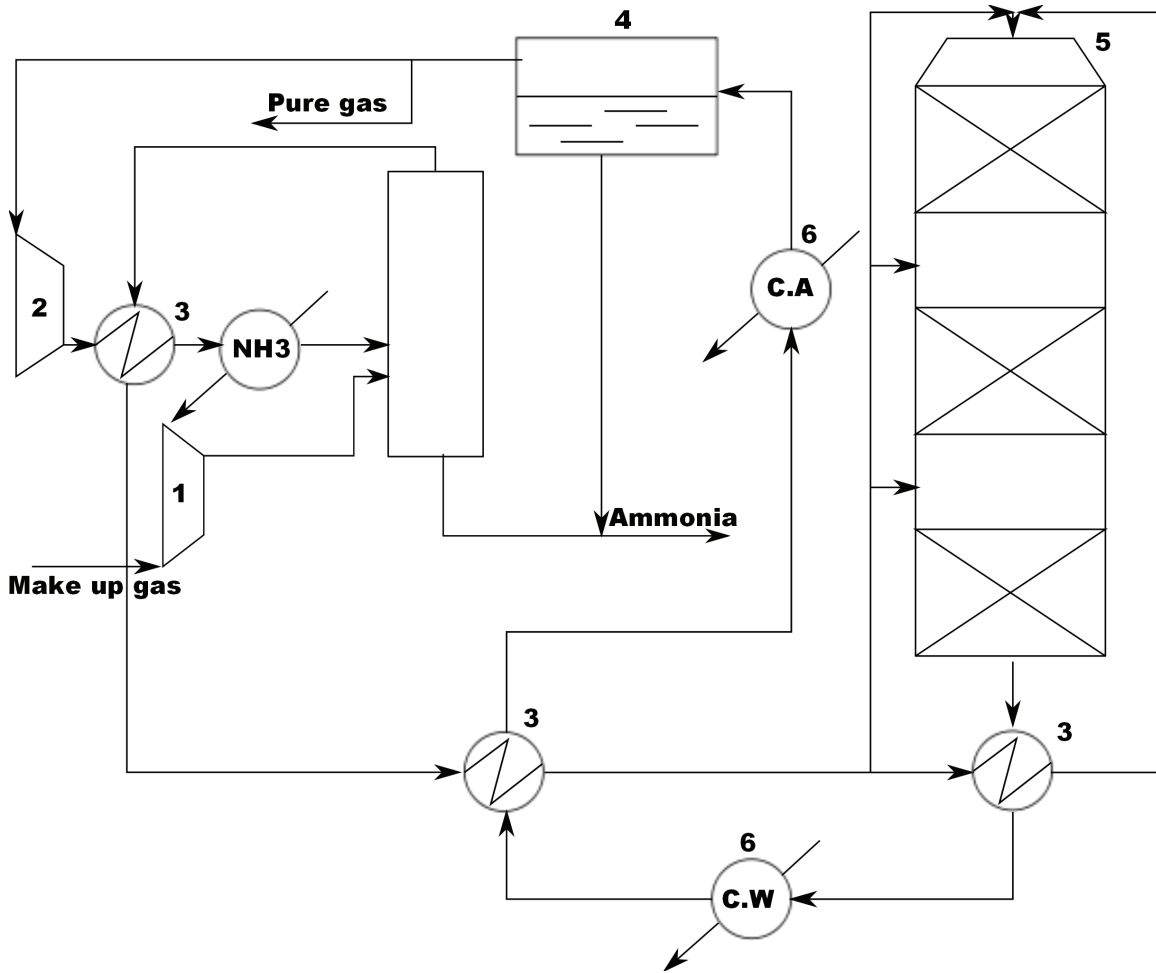


Figure 2.1: Ammonia synthesis loop with a fixed-bed quench cooling reactor; 1-compressor, 2-circulator, 3-heat exchanger, 4-separator and 5-fixed bed reactor.6-cooling.C.A-concentration ammonia. C.W-concentration water.

Following the synthesis it can be seen that the produced ammonia is removed from the gas, the unconverted synthesis gas is supplemented with fresh make up gas and the mixed recycle gas is fed back to the reactor. A compressor compensates for the pressure drop which occurs as a result from flowing the circulating gas through the piping and the auxiliary equipment. Cooling the gas mixture below its dew point and withdrawing the condensed liquid serves to recover ammonia from the recycle gas. The fresh make up gas may contain small quantities of inert components, e.g., methane and argon. The concentration of inerts in the loop is controlled to the desired level by withdrawing a small side stream, the purge gas.

The reactor shown in the figure is an adiabatic fixed bed reactor with fresh feed

quenching between the beds. Fixed bed reactors are often preferred by the industry because of their simple technology and easy operation. It is the reactor shown, including heat integration, which is the starting point of this assignment.

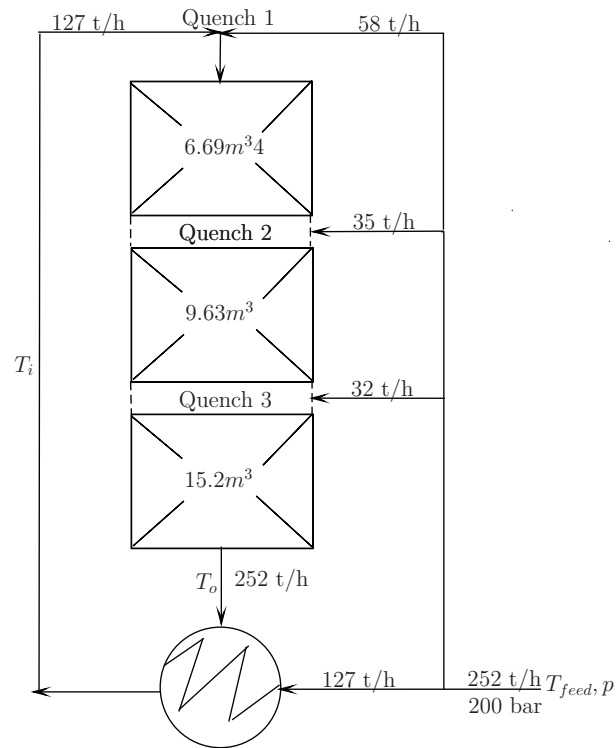
The reactor model equations are given in the Section 2.2 and are based on the reactor model from John Morud's Dr. Ing thesis: In a study of: The Dynamics of Chemical Reactors with Heat Integration. The numerical values are also taken from Morud [Mor96].

The kinetics are developed by Gintas Jouny[Juo97] as part of his diploma work and are taken from his master thesis. He replaced the original kinetic expression in the reaction equations by the Tempkin-Pyzhev equation (see, e.g., Froment and Bischohn[GK90]). He claimed that the Tempkin-Pyzhev kinetics are best suited for the simulations, because of the high operating pressure and the high ammonia inlet concentration. The kinetics are given in Section 2.2.2 and the modeling of quench points are given in Section 2.2.3. Section 2.3 and 2.4 describes the model of the heat exchanger and bypass valve respectively. At the end of the chapter, a state-space model of the system is given.

2.2 Reactor Model

As stated in the introduction, an adiabatic quenched bed reactor is used in the current work and simulations. The model is kept simple since the main concerns in this thesis are on the control design preventing the instability in occurring and not to reproduce the oscillations with great numerical accuracy. Figure 2.2 represents the ammonia reactor. Some of the parameters used in the simulations are shown for convenience.

It can be seen from the figure that the fresh feed is preheated by the reactor effluent. This is how the system maintains the high temperature needed to provoke the reaction. T_o is the reactor outlet (reactor effluent) and T_{feed} is the temperature feed. T_i is the reactor inlet temperature ,i.e., outlet temperature of the heat exchanger.



2

Figure 2.2: Ammonia synthesis reactor

2.2.1 Mass and Energy Balance

The mathematical model of the ammonia reactor consists of one model for each bed. Each bed is described by a mass and energy balance, and is discretized into ten segments. J. Morud[Mor96] has used the following assumptions applied for each segment:

- Axial flow only
- The gas temperature equals the catalyst temperature
- Constant cross-sectional gas velocity
- There is no variation in temperature, pressure or composition across the section

The assumptions are pursued in this thesis. Based on a mass and energy balance, the following partial differential equations are obtained:

$$\frac{\partial c}{\partial t} + u_w \frac{\partial c}{\partial z} = \frac{C_p}{C_{pc}} r(T, c) \quad (2.1)$$

$$\frac{\partial T}{\partial t} + u_w \frac{\partial T}{\partial z} = \frac{(-\Delta H_{rx})}{C_{pc}} r(T, c) + \Gamma \frac{\partial^2 T}{\partial z^2} \quad (2.2)$$

where:

t	Time	[sec.]
z	Position in reactor	[-]
T	Particle temperature	[K]
c	Concentration of ammonia	[kg NH ₃ /kg gas]
u _w	Migration velocity of temperature wave	[1/s]
−Δ H _{rx}	Heat of reaction	[J/kg.NH ₃]
C _{pc}	Heat capacity of catalyst and gas	[J/kg cat.K]
C _p	Heat capacity of gas	[J/kg.K]
r(T, c)	Reaction rate	[kg.NH ₃ /kg cat.sec.]
Γ	Dispersion coefficient due to finite heat transfer	[1/sec]

The mass balance given in 2.1 differs from the one found in Morud[Mor96] and in Skogestad[SM98]. The change still gives the same simulation results, but made the model in Simulink run faster. The model equations (Equation 2.1 and 2.2) can be solved as shown in Appendix B.

2.2.2 Ammonia Synthesis

Ammonia is produced on the basis of hydrogen and nitrogen, using the Haber-Bosch process (reference is made to Gniffke[Pat10]) and the reaction is highly exothermic². The reaction rate which enters Equations 2.1 and 2.2 is based on the synthesis from the elements:



This is by far the most important method for manufacturing ammonia. The kinetics used in the synthesis are developed by Gintas Jouny[Juo97] and assumes no inert and stoichiometric mixture of N₂ and H₂. The reaction rates used are:

$$r_{N_2} \rho_{cat} = k_1 p_{N_2} \left(\frac{p_{H_2}^3}{p_{NH_3}^2} \right)^\alpha - k_{-1} \left(\frac{p_{NH_3}^2}{p_{H_2}^3} \right)^{1-\alpha} \quad (2.4)$$

where $\alpha = 0.5$. The values of k_1^o and k_{-1}^o are given as:

$$k_1^o = 1.79 \times 10^4 \exp \frac{87090}{RT} \quad (2.5)$$

and

$$k_{-1}^o = 2.57 \times 10^{16} \exp \frac{198464}{RT} \quad (2.6)$$

The parameter values are taken for G. Jounys master thesis[Juo97] (Originally taken from Froment and Bischohn[GK90] p.433).

In G.Jounys work these parameter values were multiplied by a factor $k=4.75$, i.e., $k_1 = k k_1^o$ and $k_{-1} = k k_{-1}^o$. The coefficient k takes into account the differences in catalyst activity and was adjusted in order to match the industrial data of John Morud[Mor96]. G.Jouny[Juo97] states that the synthesis reaction rate expression is very important in order to reproduce the industrial reactors behavior. The modifications are pursued in the simulations given in this thesis. This is because it was the only kinetic equations which were available and since it was claimed that they were best suited- because of the high operating pressure and the high ammonia inlet concentration- for the simulations.

2.2.3 Modeling of Quench Points

Fresh feed quenching of the ammonia concentration are entering the reactor between each bed. The mixing of streams at the quench points for temperature and concentration, were modeled as follows:

$$T_{mix} = \frac{\dot{m}_b}{\dot{m}_b + \dot{m}_q} T_b + \frac{\dot{m}_q}{\dot{m}_b + \dot{m}_q} T_q \quad (2.7)$$

²An exothermic reaction is a chemical reaction that releases energy in the form of heat.

$$c_{mix} = \frac{\dot{m}_b}{\dot{m}_b + \dot{m}_q} c_b + \frac{\dot{m}_q}{\dot{m}_b + \dot{m}_q} c_q \quad (2.8)$$

The subscript q, b and mix refer to the quench stream, the reactor flow before the quench and the reactor flow after the quench, respectively. Temperature, concentration of ammonia and mass flow is denoted T, c and \dot{m} . Note that $\dot{m}_{mix} = \dot{m}_b + \dot{m}_q$ is the reactor flow after the quench.

The fresh feed quenching between each bed is used in order to maintain a reasonable chemical equilibrium (see, e.g., Froment and Bischohn[GK90]) such that the tremendous amount of heat evolved during the reaction does not damage the catalyst.

2.3 Model of Heat Exchanger

The model of the heat exchanger is also taken from John Morud's Dr.Ing. thesis [Mor96] and is originally based on equations given in Kreith and Bohn[KB86]. The feed-effluent heat exchanger was modeled with an ϵ -NTU (Number of Transit Units) model, without dynamics. For constant flow rates this reduces to a linear relation between in- and outlet temperatures when the fluid capacity is assumed constant. The relationship which follows is:

$$T_i = \epsilon T_o + (1 - \epsilon) T_{feed} \quad (2.9)$$

Where T_i and T_o is the reactor in- and out-let temperature, respectively. The heat exchanger efficiency, denoted as ϵ , is a constant between 0 and 1 and is independent of temperature. $\epsilon=0.629$ is used in the simulations by Morud[Mor96]. The relations between the heat transfer rate and the hot and cold inlet temperatures through the heat exchanger are given by the equations:

$$C^* = \frac{\dot{m}_{cold}}{\dot{m}_{hot}} \quad (2.10)$$

$$NTU = \frac{UA}{\dot{m}_{cold} C_{cp}} \quad (2.11)$$

$$\epsilon = \frac{1 - \exp -NTU(1 - C^*)}{1 - C^* \exp -NTU(1 - C^*)} \quad (2.12)$$

$$Q = \epsilon \dot{m}_{cold} C_{pg} (T_{hot,in} - T_{cold,in}) \quad (2.13)$$

$$T_{hot,out} = T_{hot,in} - \frac{Q}{\dot{m}_{hot} C_{pg}} \quad (2.14)$$

$$T_{cold,out} = T_{cold,in} + \frac{Q}{\dot{m}_{cold} C_{pg}} \quad (2.15)$$

where:

A	Heat transfer area	$[m^2]$
C^*	Ratio of flow rates	$[-]$
C_{pg}	Gas heat capacity	$[J/kgK]$
\dot{m}_{cold}	Mass flow, cold stream	$[kg/s]$
\dot{m}_{hot}	Mass flow, hot stream	$[kg/s]$
Q	Heat transfer rate	$[W]$
NTU	Number of Transfer Units	$[-]$
$T_{cold,in}$	Cold stream temperature entering heat exchanger	$[K]$
$T_{cold,out}$	Cold stream temperature leaving heat exchanger	$[K]$
$T_{hot,in}$	Hot stream temperature entering heat exchanger	$[K]$
$T_{hot,out}$	Hot stream temperature leaving heat exchanger	$[K]$
U	Heat transfer coefficient	$[W/m^2K]$
ϵ	Heat transfer efficiency	$[-]$

By comparing Equation 2.14 and 2.15 with Figure 2.2 it can be seen that the temperature feed (T_{feed}) is the cold stream and the reactor outlet temperature (T_o) is the hot stream entering the heat exchanger, i.e., reactor effluent. T_{ho} is the hot stream leaving the heating exchanger and T_i is the cold stream temperature leaving the heat exchanger.

Appendix A contains the numerical values for the parameters used for the heat exchanger, as well as other numerical key values.

2.4 ‘Bypass Valve’

The position of a bypass valve is going to be used as manipulated variable in the simulations given in Chapter 5. The valve is placed as shown in Figure 2.3 and will control the amount of cold stream mass flow entering the heat exchanger. That is, the valve splits the mass flow through the first quench into two streams. \dot{m}_c is the mass flow that enters the heat exchanger and which is being preheated by the mass flow exiting the reactor outlet. Q_1 is the second stream which bypasses the heat exchanger to the first quench where it is being mixed with the preheated mass flow exiting the heat exchanger. The bypass flows are modeled as follows:

$$\dot{m}_c = \dot{m}_1(k_0 - k_1u_1) \quad (2.16)$$

$$Q_1 = \dot{m}_1((1 - k_0) - k_1u_1) \quad (2.17)$$

where \dot{m}_c is the mass flow entering the heat exchanger. Q_1 is the mass flow, with temperature equal to T_{feed} , which enters quench 1. $\dot{m}_c = \dot{m}_c + Q_1$ is the mass flow

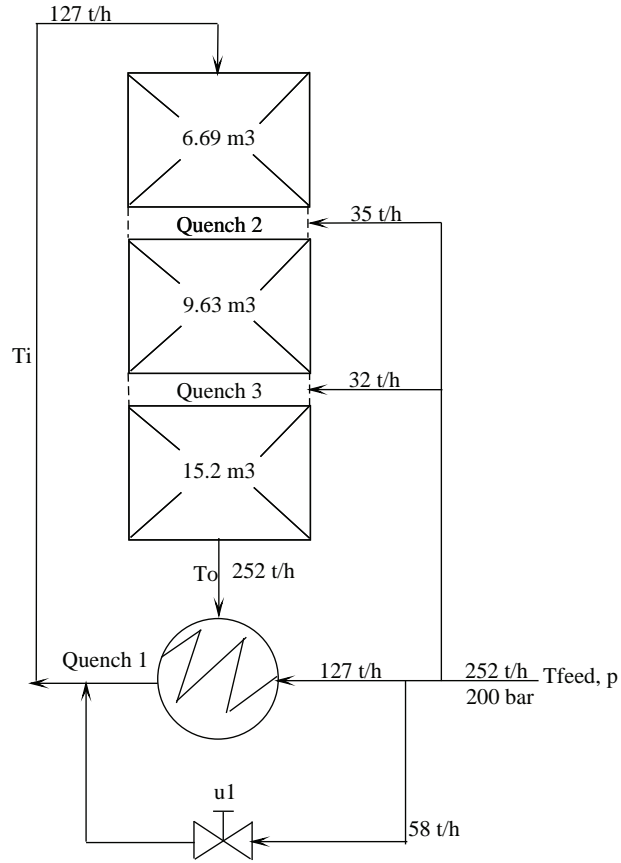


Figure 2.3: Ammonia synthesis reactor including bypass valve

entering the reactor inlet (T_i). u_1 is the valve position (manipulated variable) and k_0 and k_1 are constants. Choosing $k_0=0.5$ and $k_1=1$ gives:

$$\dot{m}_c = \frac{\dot{m}_1}{2} - \dot{m}_1 u_1 \quad (2.18)$$

$$Q_1 = \dot{m}_1 u_1 \quad (2.19)$$

which will mean that u_1 can vary between the following boundaries:

$$-0.5 \geq u_1 \leq 0.5 \quad (2.20)$$

where $u_1=-0.5$ refers to the situation where the valve is completely closed, i.e., all the mass flow ($\dot{m}_1 = \dot{m}_c + Q_1$) enters the heat exchanger. On the contrary, $u_1=0.5$ is the situation where the valve is open (all the flow bypasses the heat exchanger).

The resulting Simulink blockdiagram; including reactor with heat integration, quench points and bypass valve is shown in Figure 2.4.

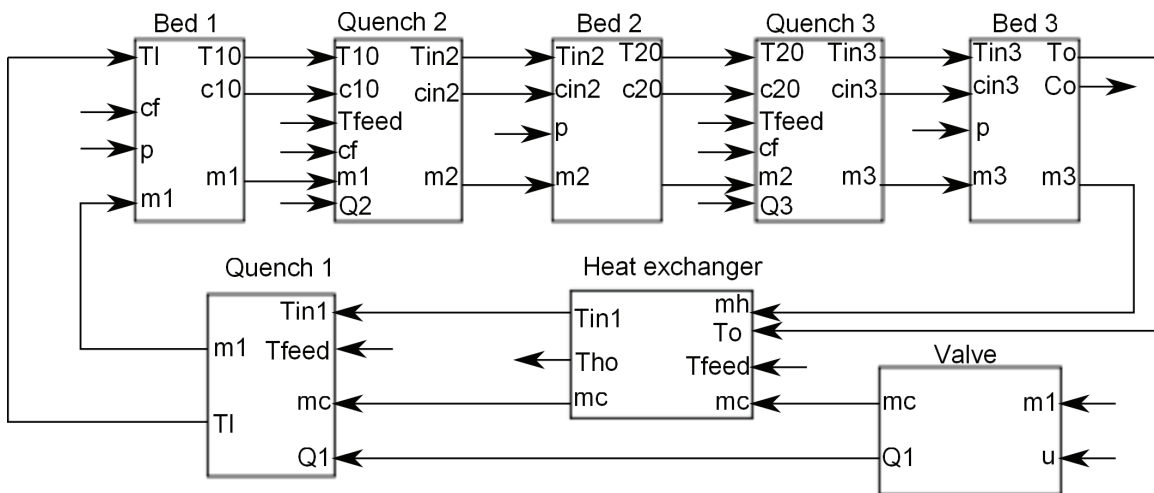


Figure 2.4: Simulink blockdiagram of reactor including heat integration and bypass valve

2.5 State-space Model

For later use a state-space model and transfer functions are developed. The two variables which are chosen as disturbances are temperature feed (T_{feed}) and reactor pressure (p). The justification of choosing these two variables will be shown by simulations in the subsequent chapters. The influence pressure and temperature feed have on the system will be dealt with in Section 6.2. These variables are also the one used in the studies by Morud[Mor96], Skogestad et.al.[SM98] and Jouny[Juo97]. The disturbances are only entering the system one at a time. Other variables which can have influence on the reactor in face of stability is dealt with in the discussion (Chapter 6).

The model of the reactor (with heat integration) was linearized numerically about at the upper (desired) operating point, yielding a state space model on the form:

$$\dot{x} = Ax + Bu + B_d d, \quad y = Cx + Du \quad (2.21)$$

Containing 30 states and where x consists of temperatures along the bed; u is the inlet temperature to the first bed (before the first quench) and y is the reactor outlet temperature, i.e., outlet temperature out of the third bed. d consist of the disturbances temperature feed (T_{feed}) and pressure (p).

The transfer function (G) and disturbance transfer function (G_d) is then given by:

$$G = C(sI - A)^{-1}B \quad (2.22)$$

$$G_d = C(sI - A)^{-1}B_d \quad (2.23)$$

The disturbance transfer function yields a MISO system with one transfer function from input "pressure" to output T_o (reactor outlet temperature) and one transfer function from input "Tfeed" (Temperature feed) to output T_o .

It is worth noting that the linearized model is stable when the heat exchanger is excluded. The linearized model which includes the heat exchanger is also stable, except when it is linearized in the range $T_{\text{feed}}=232\text{-}224$ °C or at pressure, p=162-171 bar.

A thorough analysis for the case when the reactor model is linearized without the heat exchanger can be found in Morud[Mor96], Morud and Skogestad[SM98] or Jouny[Juo97].

Appendix C constains the MATLAB script used to create the statespace realization.

Chapter 3

Control of Reactor

3.1 Introduction

Some issues have to be mentioned before we embark on the control of the ammonia reactor in question. First, John Morud found in his Dr. Ing. thesis [Mor96]-based on a steady state characteristic- that the ammonia reactor has three operating points, where we mainly are concerned with the upper one. The upper operating point possesses the highest temperature, which leads to the highest conversion of ammonia. The rate of the reaction at lower temperatures is extremely slow, so a higher temperature must be used to speed up the reaction rate, although it results in a lower yield of ammonia.

The lowest operating point corresponds to extinction. When this happens, the reactor can not resume to normal operation without external addition of heat and because of this, we do not want to operate at this steady state operating point.

Secondly, the oscillations given in Figure 3.1 in Section 3.2- produced by the drop in pressure or temperature feed- may lead to material damage in the reactor and deterioration of the catalysts. Thus, there are two different reactor behaviors which want to be avoided by controlling the ammonia reactor.

Third, it is a fact that many reactors in the industry are left uncontrolled. When a process unit on sight can operate safely without control, this is often preferred by the engineers, as they generally wish to keep the complexity of the plant to a minimum. It is well known that plant management and operators prefer manual operation. The economic benefits by keeping the plant complexity to a minimum is often one of the main reasons, since applying a more advanced controller structure is more expensive, time-consuming and requires in-plant training of personnel. So, in dealing with control of chemical reactors, simple controllers are more likely to be favored.

When it comes to the issue of controlling ammonia reactors, the need for a high

margin of stability is traded off by the need for optimal production in the synthesis loops. The maximum production rate is obtained in a state where the steady state stability margin is small.

Before the control issues of the ammonia reactor are addressed, the sustained oscillations which formed the basis of John Morud's Dr.Ing; "The Dynamics of Chemical Reactors with Heat Integration", and the paper written by Skogestad and Morud [SM98]; "Analysis of instability in an industrial ammonia reactor", are recreated.

3.2 Open-loop Simulations

There are basically two ways to obtain the sustained oscillations when the ammonia reactor operates in open-loop. The first one is by a decrease in temperature feed. Morud [Mor96] found out that when the temperature feed drops below the critical value: $T_{\text{feed,crit}}=235.2$ °C, the system becomes unstable and exhibits sustained oscillations. This result is verified by Figure 3.1, where the temperature is decreased by 10 degrees °C every fiftieth minute, starting at $T_{\text{feed}}=250$ °C. It can be seen from the figure that the outlet temperature remains stable until it drops down to 230°C. The pressure in the ammonia reactor were kept constant at 200 bar during the simulation.

The second way to obtain the oscillations is by a decrease in pressure. Sigurd Skogestad and John Morud[SM98] has shown in their paper that a drop in pressure below 170 bar will also result in sustained oscillations in the reactor temperature (the critical value was found to be $p_{\text{crit}}=172$ bar). During this simulation, the temperature feed (T_{feed}) was kept constant at 250 °C. The instability is verified by simulation and shown in Figure 3.2.

It can be seen from the figure that the reactor outlet temperature is stable with a pressure of 200 bar and that it remains stable when the pressure drops down to 170 bar; and settles at a new steady state with a lower temperature, though with small oscillations. The oscillations begin after fifty minutes, when the pressure is further decreased down to 150 bar. The figure also shows that the temperature at the reactor outlet stabilizes and recovers to its original steady state when the pressure is increased back to 200 bar. This also applies when temperature feed is the influencing disturbance.

It is well known that the presence of RHP-zeros implies high gain instability. In a study of: "The Dynamics of Chemical Reactors with Heat Integration", John Morud [Mor96] found that the Nyquist- and Bode- plots can be used to predict the point of instability. He also states that the phenomena occurs when a pair of complex poles (eigenvalues) crosses into the right half plane, due to the presence of the RHP-zeros. That is, the transfer function from reference to the plant input approaches the inverse

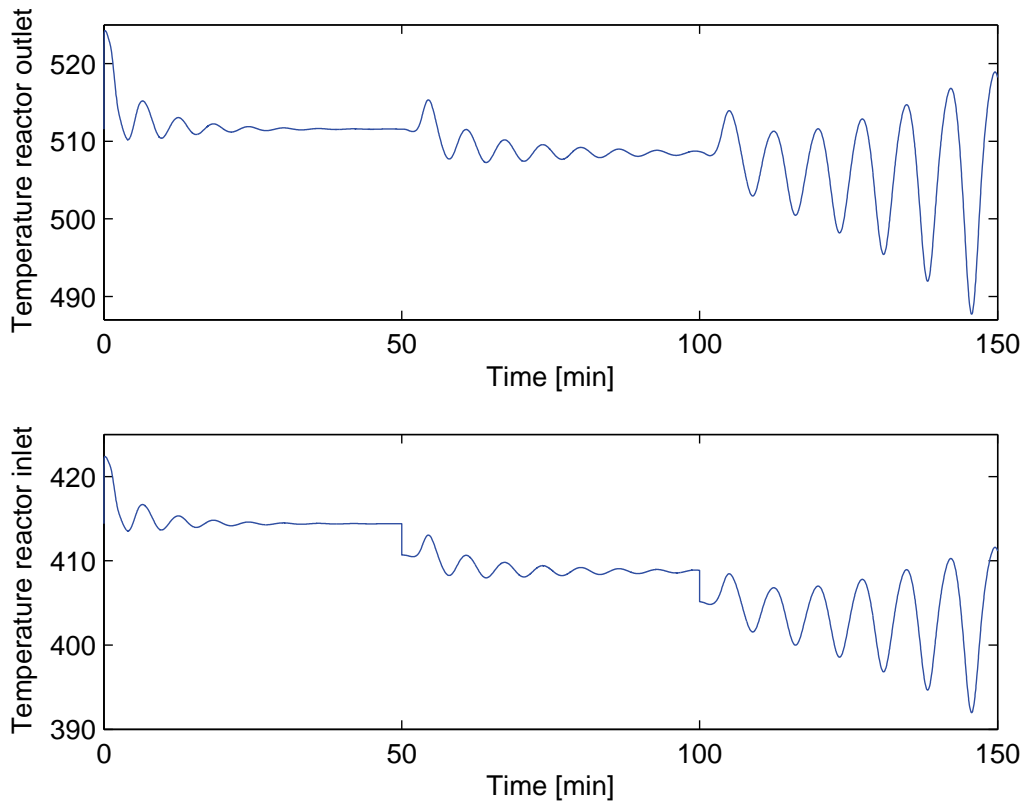


Figure 3.1: Nonlinear simulation of a drop in feed temperature (T_{feed}). Initial temperature is 250 °C, decreases to 240 °C (at $t=50$) and drops down to 230 °C ($t=100$)

of the plant. The result is that the RHP-zeros eventually appear as unstable poles in the closed-loop system, if the bandwidth is too high.

The physical explanation of the instability can be described as two independent waves traveling through the reactor, one temperature wave and one concentration wave. The two waves travel at different velocities. The concentration wave travels at approximately the chemical species velocity. The temperature wave, on the other hand, travels at a slower velocity which is dependent on the thermal properties of the fluid and catalyst.

Consider one fixed bed, divided into ten segments, where the exothermic reaction of ammonia is taking place. Assume that a sudden decrease in the feed temperature (T_{feed}) occur (negative step change). The immediate effect of the temperature feed drop is a decrease in the reaction rate in the first segments of the bed. Because the temperature wave travels at a slow velocity, the immediate effect on the last

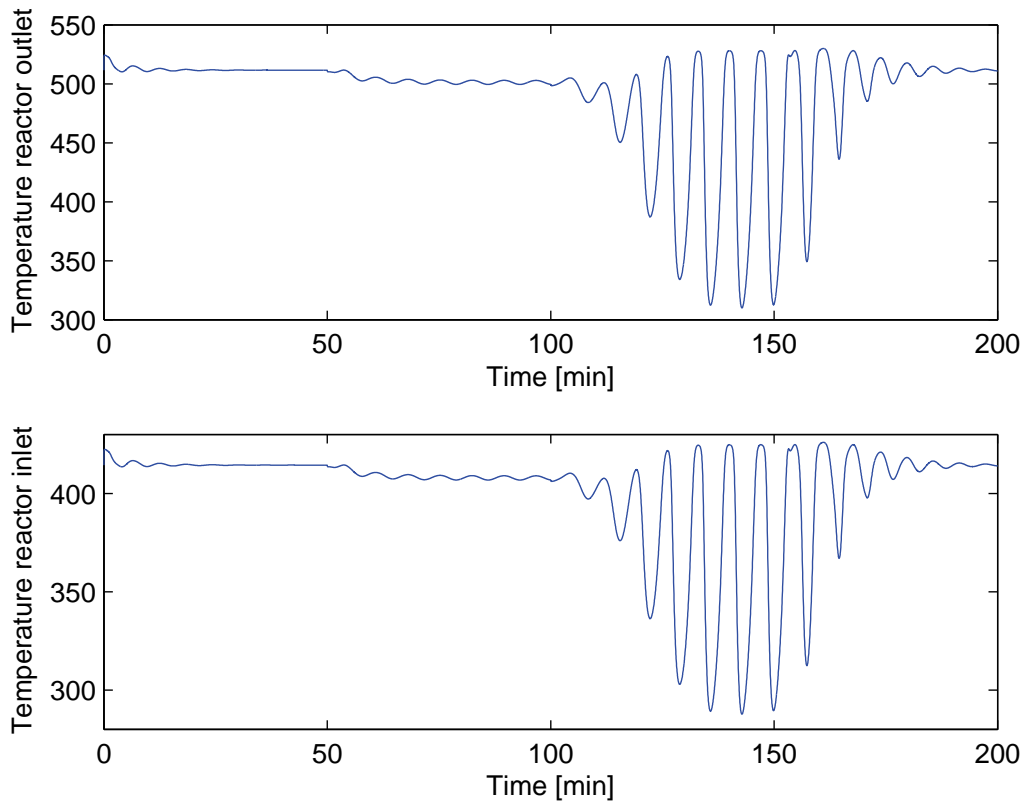


Figure 3.2: Nonlinear simulation of decrease in the reactor pressure from 200 bar to 170 bar (at $t=50$), further down to 150 bar (at $t=100$) and back to 200 bar (at $t=150$)

segments in the bed is to make the ammonia concentration higher, so that the temperature in the last part of the bed increases. In the end, there is a loss of conversion in the entire bed and the outlet temperature begins to decrease (reference is made to Morud[Mor96]). This inverse response is the reason why the reactor temperature starts to oscillate, instead of leading to the more common problem of extinction.

The oscillations may just be caused by a sudden pressure drop (as shown in Figure 3.2) in the synthesis loop and the presence of the RHP-zeros is still the reason why the reactor temperature begins to oscillate.

RHP-zeros appear usually when the system contains competing effects of fast and slow dynamics, which can be recognized in the explanation given above. That the ammonia model then contains several RHP-zeros is not surprising.

This section has shown that the reactor temperature will start to oscillate when the temperature feed (or pressure) decreases. The simulation results when feedfor-

ward and feedback are included are given in Chapter 5.

3.3 PID-controller

As stated in the introduction of this section, simple controllers are almost always favored in control of chemical reactors. The controllers used in this thesis are therefore kept simple. It is well known that PID-controllers are favored in the process industry. The controllers given in the subsequent sections are based on the PID-controller equation:

$$K_{PID}(s) = K_c \left(1 + \frac{1}{K_i s} + K_d s \right) \quad (3.1)$$

which is on (ideal) parallel form. The reason for using the ideal form is simply because that the cascade implementation is less general and does not allow for complex zeros (reference is made to Skogestad and Postletwaithe[Sko03]). K_c , K_i and K_d are the proportional gain, integral time and derivative time, respectively¹

3.4 P-controller and the Reactor Inlet Temperature as Measurement

John Morud ([Mor96]) proposes in his Dr. Ing. thesis that the reactor system could be stabilized using the mass flow through the first quench to control the temperature at the inlet to the first bed. Which means using the temperature feed mass flow Q_1 as manipulated variable and the reactor inlet temperature (after the first quench) as measurement.

This is probably the most realistic way to control the reactor in a real ammonia synthesis plant. This can be done by a simple P-controller only since it is a simple mixing process at the first quench. Thus, the control loop does not contain any RHP-zeros.

Because of the inverse response (caused by RHP-zeros) positive feedback ($e=y-r$) is included. This is obtained by making the proportional gain negative. The proportional gain during the simulations were $K_c=-0.1$.

The simulation results with this controller and controller structure applied is given in Section 5.1.

The observed RHP-zeros phenomena described by Morud[Mor96] may be a limitation of the performance of the reactor (including heat integration) when the purpose is to control the reactor outlet temperature (T_o), or some other internal temperature

¹ K_i and K_d are used instead of the conventional use; T_i and T_d . This is done to avoid confusing it with the reactor inlet temperature, which is denoted T_i in this thesis.

in the reactor, e.g., the temperature outlet of the first or second bed, using a quench further upstream in the reactor as manipulated variable.

The above mentioned way to control the reactor is how we want to control the reactor in the rest of this thesis and this is described in the next section.

3.5 PD-controller and the Reactor Outlet as Measurement

As already stated, the reactor system contains several RHP-zeros. It is well known that RHP-zeros generally correspond to inverse response behavior in the time domain (see, e.g., Skogestad and Postlethwaite [SP07]). This is also verified by the nonlinear simulations given in Section 5.2. Such RHP-zeros will (usually) pose a limitation for control.

The oscillations appear as a result of too low inlet temperature through the ammonia reactor. To avoid the instability, one can naturally increase the inlet temperature, T_{feed} , or the reactor pressure (p).

Another possibility is to increase the heat recovery by reducing the flows through one of the other quenches (Q_1, Q_2, Q_3) so that more of the feed is preheated. The drawback with this is that it can only be done to a limited extent, i.e., if the quench valve saturates (becomes completely closed), there will be no possibility to increase the temperature, and thus enabling the possibility for extinguishing the reactor (reference is made to Section 3.1). Despite the drawback, this is how the ammonia reactor is going to be controlled in this section. That is, using the mass flow through the first quench to stabilize the reactor outlet temperature (T_o).

The reason for choosing to control the mass flow through the first quench is because it is the quench where the largest amount of mass flow enters the reactor². And hence, one would expect that the first quench has most effect on the reactor temperature.

The controller applied during the simulations is a PD-controller. A simulation experiment, done by my supervisor Professor Morten Hovd, revealed that a pure PI-controller could not stabilize systems on the form:

$$G(s) = \frac{1}{s^2 + a \cdot s + b}, \quad \text{for } b > 0, \quad a < 0 \quad (3.2)$$

Derivative action must be included to get smaller negative phase shift around the cross-over frequency (PD- or PID-controller).

²Based on the industrial data found in Morud[Mor96]

The simulations of the reactor model revealed that it is not possible to stabilize the reactor with integral action included. Including integral action resulted in negative mass flow through the first quench, for the case when no constraints were applied to the input. The result was immediate saturation, when constraints were applied to the input. The tuning method applied for the PID controller was SIMC³.

The controller applied to the plant was then a PD-controller. The controller parameters applied are $K_c=-0.009$ and $K_d=0.001$. It is not possible to keep the manipulated variable between its limitations if one chooses controller parameters with a higher value. The negative proportional gain is still used to get the positive feedback. By increasing the proportional gain and/or the derivative action resulted in instability and extinction.

³The Ziegler-Nichols tuning were also applied, with the same results

Chapter 4

Feedforward Design

4.1 Introduction

This chapter describes how feedforward can be used to reduce the magnitude of the input moves, which will then prevent instability caused by input constraints. The feedforward design in this chapter is based on the description given in; Feedforward for stabilization, written by M.Hovd and R.Bitmead [HB07].

Reading through the paper; feedforward for stabilization, one find different results on how to obtain the minimal achievable H_∞ -norm. One such result is:

$$\|KS\|_\infty = 1/\underline{\sigma}_H(\mu(G)^*) \quad (4.1)$$

where $\underline{\sigma}_H$ denotes the smallest Hankel singular value, $S = (I + KG)^{-1}$ and $\mu(G)^*$ denotes the anti-stable part of the plant model G with its RHP-poles mirrored into the LHP. This result was first shown by Glover[Glo86] and a extension of Glover's result which includes the disturbance model can be found Kariwala[Kar04]. Simplifications of these results can be found in Skogestad and Postlethwaite[SP07].

The bound given in Equation 4.1 tells us that the peak on the transfer function is required to be small in order to avoid large input signals when the system is influenced by disturbance(s) and noise. A large value of the bound in Equation 4.1 will make the input saturate and thereby making stabilization difficult.

In order to make the relationship given Equation 4.1 to have any relevance for evaluating input saturation, the model used (G and/or G_d) must be properly scaled. Skogestad and Postlethwaite[SP07] recommends scaling the plant input such that: For any reference r between $-R$ and R and any disturbance d between $-1 \geq d \leq 1$, will keep the output (y) within the range $r - 1 \geq r \leq 1$ (at least most of the time), using an input within the range $-1 \geq u \leq 1$ (reference is made to Skogestad and Postlethwaite[SP07] p. 5-6).

The subsequent sections will describe two different approaches of how the introduction of feedforward can minimize the input usage and thereby obtain closed-loop stability. Section 4.2 describes the implementation using a stable disturbance model and Section 4.3 describes the implementation with an unstable disturbance model.

4.2 Stable Disturbance Model

The ammonia reactor is unstable from input to output, and therefore it requires feedback control for stabilization. The disturbance model, however, is stable when it is linearized around $T_{\text{feed}}=240\text{-}250\text{ }^\circ\text{C}$. This section shows how the feedforward design can be implemented when the disturbance model is stable. The disturbance model is linearized around $T_{\text{feed}}=250^\circ\text{C}$ during the design procedure given below, and in the simulations given in Chapter 5.

Consider the control structure given in Figure 4.1. Without the feedforward element ($K_f=0$), this is the structure of the reactor system:

With the feedforward element active ($K_f \neq 0$) and assuming that the saturation

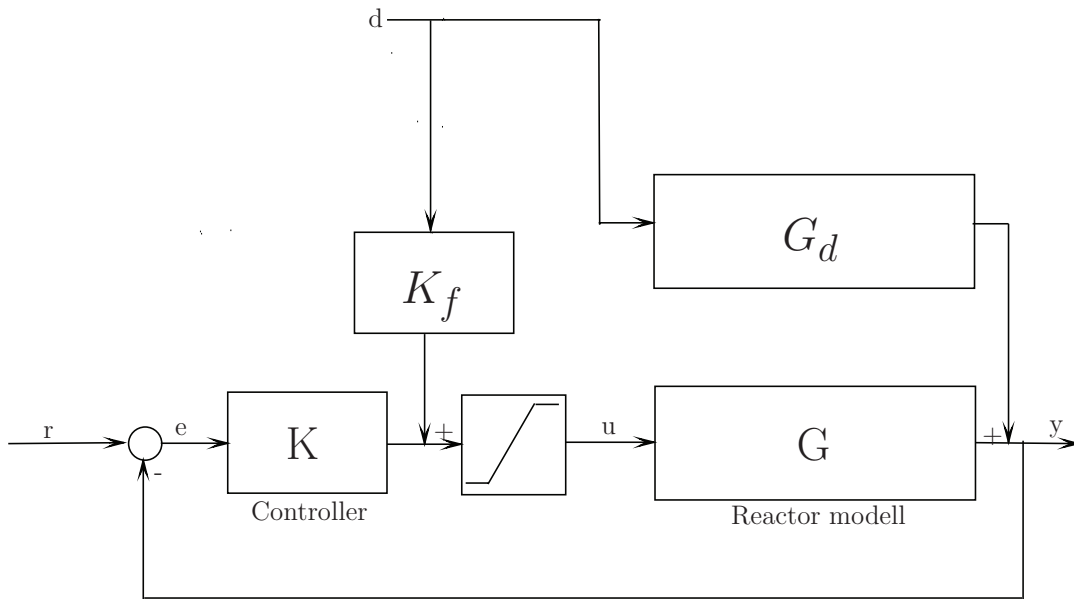


Figure 4.1: Blockdiagram

element is inactive we get the following:

$$u = K S r + S(K_f - K G_d) d \quad (4.2)$$

where $S = (I + KG)^{-1}$, which is true for SISO-systems¹. Introducing the feedforward element in Equation 4.2 gives a new degree of freedom for minimizing the input usage when disturbances enters the reactor system. The conventional form of the feedforward element (K_f) is the following:

$$K_f = -G_d G^{-1} \quad (4.3)$$

but the feedforward given in Equation 4.3 cancels the effect on the disturbance on the output. Instead, we would like to find a feedforward element which cancels the effect of the disturbance on the input. Reference to Morten Hovd and R. Bitmead[HB07] reveals that the feedforward element, K_f , should have the following form:

$$K_f = KG_d \quad (4.4)$$

From Equation 4.2 it can be seen that this feedforward element cancels the effect from the disturbance on the input.

Hovd and Bitmead[HB07] also suggest augmenting the feedforward design with a high pass filter to obtain offset-free control and shows a reformulation of the plant and disturbance transfer function when the controller contains an integrator. The simulation results, using the implementation described here, are given in Chapter 5.

4.3 Unstable Disturbance Model: A "Reference Governor" Approach

The implementation of feedforward when the plant model was unstable, but the disturbance model was stable, was given in the previous section. This section shows how to implement the feedforward design when the disturbance model is also unstable (reference is made Section 2.5 that the state matrix is unstable when its linearized in the range $T_{\text{feed}}=224-232^\circ\text{C}$ or a reactor pressure of 162-171 bar).

When the disturbance model is unstable, the conventional feedforward element in Equation 4.3 would lead to an unstable feedforward element K_f which would result in an internally unstable system.

The solution (proposed by Hovd and Bitmead[HB07]) is to find a stable feedforward element, K_f , which minimizes: $(K_f - KG_d)$ in Equation 4.2.

Hovd and Bitmead[HB07] has drawn the attention to the fact that the term KG_d should be divided into a stable and an anti-stable part:

$$KG_d = KG_{d,stable} + G_{d,unstable} \quad (4.5)$$

¹This may not be the case for MIMO-systems (Reference is made to Skogestad and Postlethwaite p.176)

the stable transfer function; $KG_{d,stable}$ can be used directly in the feedforward element, K_f . For the anti-stable transfer function; $G_{d,unstable}$, we need to find a stable approximation.

A solution to the problem of finding an approximation of an anti-stable transfer function by a stable transfer function can be found in Glover[Glo84]. Professor Morten Hovd made a MATLAB script based on the solution in Glover [Glo84], which is used to find the stable approximation of $G_{d,unstable}$ (denoted $\tilde{G}_{d,unstable}$ in this thesis).

$$K_f = KG_{d,stable} + \tilde{G}_{d,unstable} \quad (4.6)$$

which can be directly implemented, together with the model of the ammonia reactor as shown in Figure 4.1.

However, Hovd and Bitmead[HB07] proposes a simple reformulation of the feedforward arrangement, denoted: the "reference governor" approach. This rearrangement is presented in Figure 4.2. It can be seen from the figure that the transfer function

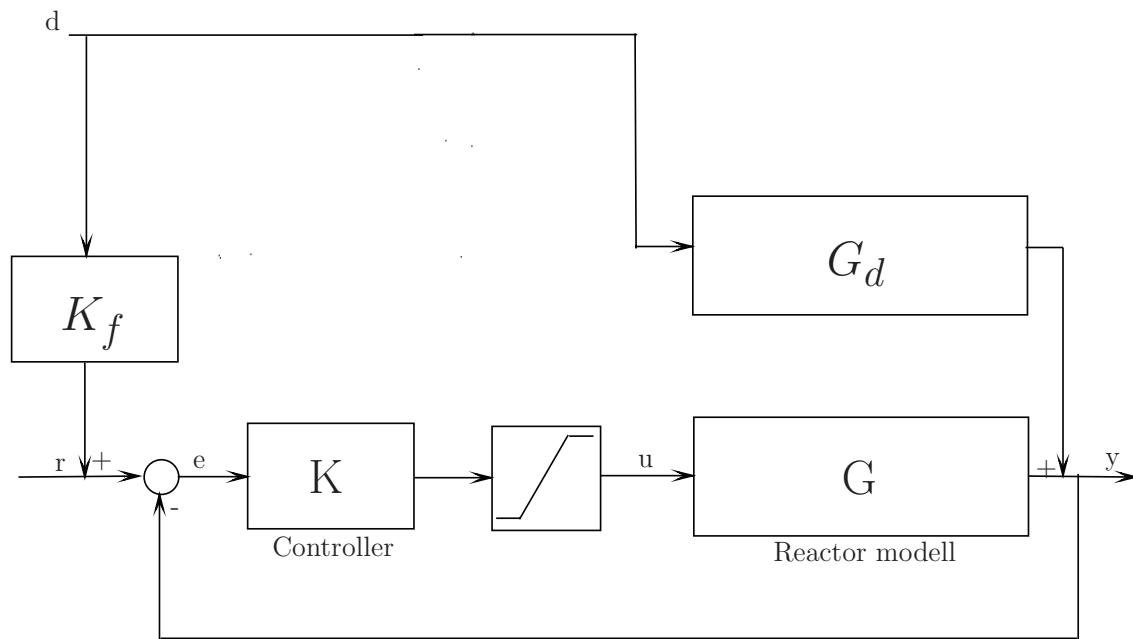


Figure 4.2: Feedforward arrangement for an unstable disturbance transfer function from the disturbance (d) to the error (e) (still assuming that the saturation element is inactive) is the following.

$$e = (K_f - G_d)Sd \quad (4.7)$$

where S still is the sensitivity function. For a given controller, Hovd and Bitmead[HB07] argues that the controller input and therefore the controller output will be small if

the term $(K_f - G_d)$ is small.

With the feedforward element implemented as:

$$K_f = G_{d,stable} + \tilde{G}_{d,unstable} \quad (4.8)$$

this can easily be realized. Where $\tilde{G}_{d,unstable}$ is the stable approximation of the anti-stable part of G_d , with the unstable poles mirrored into the left plane.

There is one weakness with the subroutine based on the solution found in Glover[Glo84]. Namely, RHP-zeros which are located close to the imaginary axis lead to a (very) large Hankel singular value (reference is made to Section 4.3.1). This results in a poor (stable) approximation of the unstable part of G_d .

From the MATLAB script given in Appendix C one can find that the RHP-poles of the A-matrix (when linearized around the upper steady state and $T_{feed}=230^\circ\text{C}$) is equal to: $0.0010 \pm 0.0142i$; And when it is linearized around $p=170$ bar, one will find that the RHP-poles are equal to: $0.0002 \pm 0.0148i$.

The RHP-poles are located close to the imaginary axis in both cases, which implies that the stable approximation, of the anti-stable part of G_d , will give a very large Hankel singular value.

In the next chapter we will try to avoid this disadvantageous situation by finding an unstable operating point where the RHP-poles are located further into the right half plane. The simulation results with this type of feedforward arrangement are given in Chapter 5.

4.3.1 Hankel -Norm and -Singular Values

A discussion concerned with Hankel singular values was given in the previous section and a further discussion is made in Chapter 5. A brief explanation of the terms Hankel -norm and -singular values are therefore appropriate. The explanation given here is based on the one given in Skogestad et. al.[SP07].

The Hankel norm is an induced norm from past inputs to future outputs and closely related to the H_∞ - norm. It can be shown that the Hankel norm is equal to:

$$\|G(s)\|_H = \sqrt{\rho(PQ)} \quad (4.9)$$

where ρ is the spectral radius, i.e., $\rho = \max|\lambda_i(A)|$ (the absolute value of the maximum eigenvalue). P and Q is the controllability and observability Gramian defined by:

$$P \triangleq \int_0^\infty e^{A\tau} B B^T e^{A^T \tau} d\tau \quad (4.10)$$

$$Q \triangleq \int_0^{\infty} e^{A\tau} C C^T e^{A^T \tau} d\tau \quad (4.11)$$

The corresponding Hankel singular values are then given by the positive square roots of the eigenvalues of the PQ-matrix:

$$\sigma_i = \sqrt{\lambda_i(PQ)} \quad (4.12)$$

where subscript i refers to the i 'th singular value of the i 'th eigenvalue. The name Hankel refers to the special structure of the PQ-matrix ,i.e., a Hankel matrix is a square matrix with constant (positive sloping) skew-diagonals.

4.4 H_{∞} -control and Feedforward

The scientific paper written by Hovd and Bitmead[HB07] also describes the use of the feedforward strategy augmented with a suboptimal H_{∞} -controller. The controller design is based on the the realization of $[G_d \ G]$ and a 2-DOF controller.

The resulting H_{∞} -control synthesis violates the assumptions A2 and A4 of Zhou et. al.[KZG96](p.450)². As compensation Hovd and Bitmead[HB07] have added a small measurement noise n and the magnitude of the noise is reduced until further reduction does not affect the H_{∞} -norm achieved. The resulting controller synthesis should be implemented as shown in Figure 4.3.

The design of the controller is not realized in this thesis. The reason is that the MATLAB script complains on the scaled realization of the system (or that it is close to singular) and MATLAB returns an empty controller.

Skogestad and Postlethwaite[SP07] states that most sensible control problems will meet the standard assumptions. On the basis of this, the reason why the controller does not work is probably because the control problem is not well formulated. Reformulation of the state-space matrices given are necessary in order to implement the controller together with the ammonia reactor. The author of this thesis did not have enough time in order to investigate which assumptions which is violated with the state-space formulation given in Section 2.5.

The H_{∞} -controller synthesis is given in Appendix C.

²The same assumptions can be found in Skogestad and Postlethwaite[SP07], i.e., A4 and A6 p.354

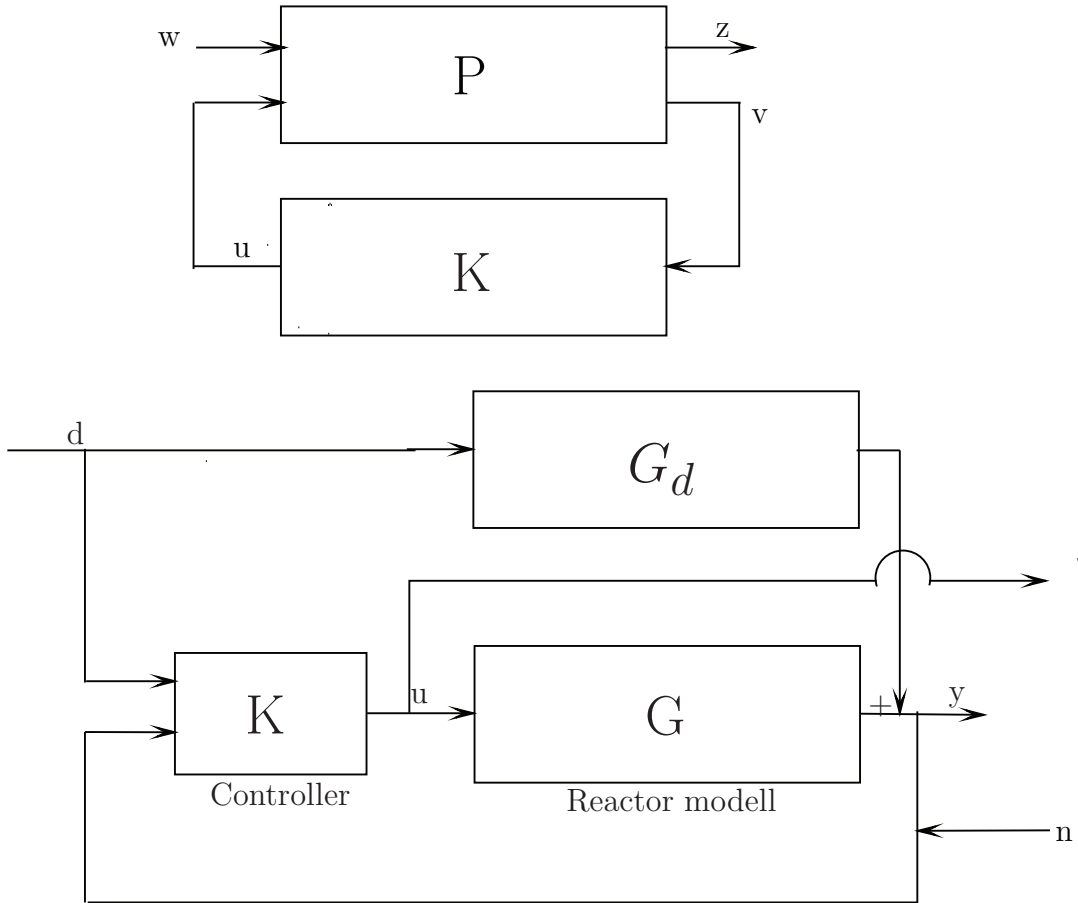


Figure 4.3: H_∞ -controller synthesis for a 2-DOF controller

Chapter 5

Simulation Results

5.1 With the Reactor Inlet Temperature as Measurement

This section shows the simulation results using the reactor inlet as measurement and shows that the RHP-zeros are not a limitation in order to stabilize the reactor system. Controlling one of the quench valves using the reactor inlet as measurement is probably how the reactor would be controlled in an actual ammonia synthesis plant.

The controller and control structure given in Section 3.4 are used during all the simulations in this section.

Section 5.1.1 presents the simulation results without constraints applied to the input. Section 5.1.2 explains why there does not exist an unstable operating point with RHP-poles further into the right half plane.

5.1.1 Unconstrained Input

Control of the ammonia reactor, without constraints on the input, is shown in Figure 5.1. The figure shows two different simulation results; one where the temperature feed (T_{feed}) is used as disturbance. In the other simulation, a reduction in the reactor pressure is the influencing disturbance. The disturbance enters the system in exactly the same way as in the open-loop simulations given in Figure 3.1. The spikes shown when temperature feed is the influencing disturbance are most likely caused by the quench modeling (reference is made to Section 2.2.3).

The figure shows that the controller stabilizes the reactor temperature when the fresh temperature feed is decreased down to 230°C. The reason for this—as also stated by John Morud in his Dr. Ing. thesis [Mor96]—is that the control loop does not

contain any RHP-zeros since it is only a simple mixing process of the first quench (reference is made to the modeling of quench points given Section 2.2.3). The ammonia reactor with heat integration will respond much like a reactor with an independent heat exchanger.

This section shows that it is possible to control the reactor with the use of a simple controller, so that stabilization of the ammonia reactor is not limited by the RHP-zeros.

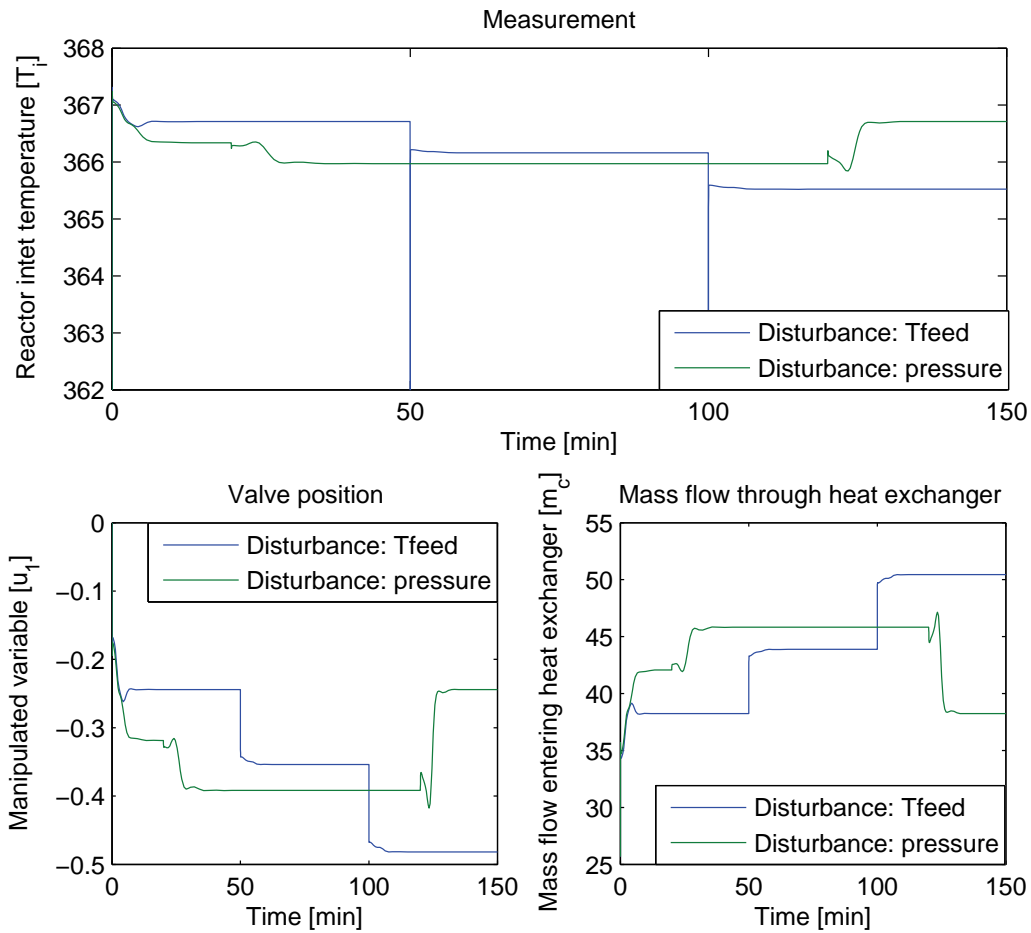


Figure 5.1: Nonlinear simulation with proportional control. The blue line represents the reactor inlet temperature when T_{feed} is the influencing disturbance. At $t=50$, T_{feed} is decreased down to 240°C ; and at $t=100$ it is further decreased down to 240°C . The green line shows the reactor inlet temperature during a decrease in reactor pressure. At $t=0$ the pressure is reduced from 200 to 170 bar. At $t=20$ the pressure is reduced from 170 to 150 bar; and back to 200 bar at $t=120$.

5.1.2 Finding an Unstable Operating Point with RHP-poles Further into the RHP

As stated in Section 4.3, the solution of finding a stable approximation of the anti-stable part of G_d used in this thesis, gives a poor approximation when the RHP-poles are located closed to the imaginary axis.

To avoid the use of the poor approximation, we will try to find an unstable operating point where the RHP-poles are located further into the right half plane. To find this operating point, simulations without constraints on the input are carried out, with larger decreases in the disturbances (pressure or temperature feed). The mass flow can not be negative during the simulations, since it would lead to an unrealistic case study.

The Figure 5.2 shows one of the simulations results. It can be seen from the figure that the manipulated variable is quite near the lower constraint. In fact, it would cross the lower constraint with a slightly larger disturbance, which is represented by the blue line in the figure.

The manipulated variable can not counter the disturbance in this situation either, the only way to stabilize the reactor is to increase the amount mass flow through the heat exchanger, but this is not possible in the situation given in Figure 5.2 since the valve is ("more than") closed.

The simulation results given in Figure 5.2 are obtained with temperature feed (T_{feed}) acting as disturbance. Similar results can be obtained with pressure as disturbance.

Another way to find an unstable operating point with RHP-poles further into the right half plane can be to reduce the mass flows through the other quenches (quench 2 and 3), i.e., increasing the mass flow through the heat exchanger. This would then no longer be the same simulation study found in Morud[Mor96], Skogestad and Morud[SM98] and Jouny[Juo97], but it is the last chance to implement the feedforward strategy as intended.

However, it turns out that reducing the other quench flows does not result in an increased freedom to control the reactor in face of disturbance. The reason is the heat exchanger model. Calculations (based on the equations given in Section 2.3) show that increasing the (cold stream) mass flow through the heat exchanger does not correspond to higher, but lower temperature at the reactor inlet (heat exchanger outlet). That is, a larger (cold stream) mass flow through the heat exchanger will result in a lower heat transfer efficiency (ϵ) which will lead to a lower temperature at the reactor inlet.

Therefore there is a trade off between making more of the (cold stream) mass flow go through the heat exchanger and making the cold stream mass flows get mixed with the reactor flow between the beds (at the quench points).

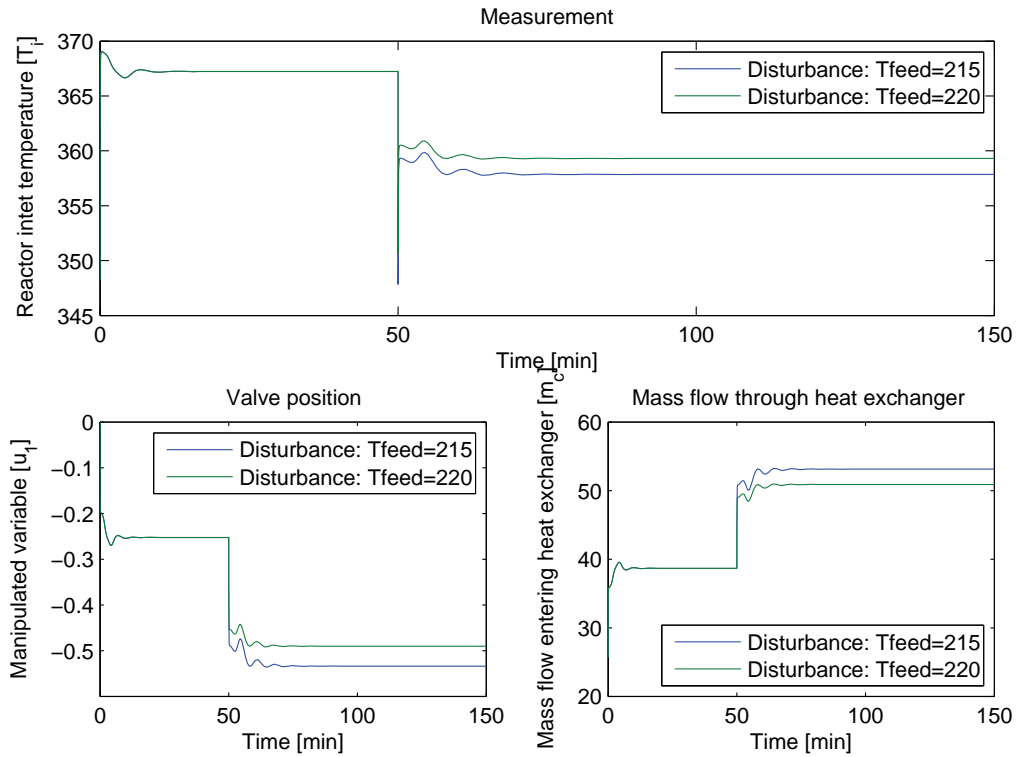


Figure 5.2: Nonlinear simulation with (large) decrease in temperature feed. The green line shows how the system reacts on the disturbance $T_{\text{feed}}=-30^{\circ}\text{C}$. The blue line shows how the system reacts for a disturbance $T_{\text{feed}}=-35^{\circ}\text{C}$. The disturbance enters the system at $t=50$ min in both simulations.

Table 5.1 shows some of the calculations. The temperature feed and the reactor outlet temperature are held constant at $T_{\text{feed}}=250^{\circ}\text{C}$ and $T_{\text{o}}=510^{\circ}\text{C}$ when the calculations are carried out. The (hot stream) mass flow out the reactor is always constant ($\dot{m}_h = 70\text{kg/s}$). Thus, the only variable which is varying is the (cold stream) mass flow entering the heat exchanger.

Table 5.1: Heat exchanger calculations

Mass flow used in Morud's study	No bypass flow	$\dot{m}_c = \dot{m}_c + Q_1 + \frac{Q_2}{2} + \frac{Q_3}{2}$
$\dot{m}_c = 35.2778\text{kg/s}$	$\dot{m}_c = 51.3889\text{kg/s}$	$\dot{m}_c = 60.69445$
$\epsilon = 0.62853$	$\epsilon = 0.48597$	$\epsilon = 0.42826$
$T_i=413.42^{\circ}\text{C}$	$T_i=376.35^{\circ}\text{C}$	$T_i=361.35^{\circ}\text{C}$

Q_k refers to mass flow of fresh temperature feed which get mixed with the reactor flow at quench k.

It can be seen from the Table 5.1 that the heat efficiency coefficient (ϵ) (and therefore also the reactor inlet temperature) decreases when the mass flow through the heat exchanger increases. The controller will (as a result of this) make the reactor temperature settle at the lower steady-state.

A shift in the chemical equilibrium may also be an explanation of why reducing the other quench flows does not result in increased reactor temperature.

5.2 With the Reactor Outlet Temperature as Measurement

This section shows the simulation results with the reactor outlet (T_o) as measurement. The controller used in the simulations are given in Section 3.5.

Section 5.2.1 shows the results without constraints on the input and the simulation results with constraints are given in Section 5.2.2. The simulations of the different feedforward implementations are given in the last section.

5.2.1 Unconstrained Input

Figure 5.3 shows the simulation results when the manipulated variable is not limited by constraints and the temperature feed (T_{feed}) is used as disturbance in the same way as for the results given in Section 3.2. Figure 5.4 shows the performance with pressure acting as disturbance.

It can be seen from the figures that the controller stabilizes the system when

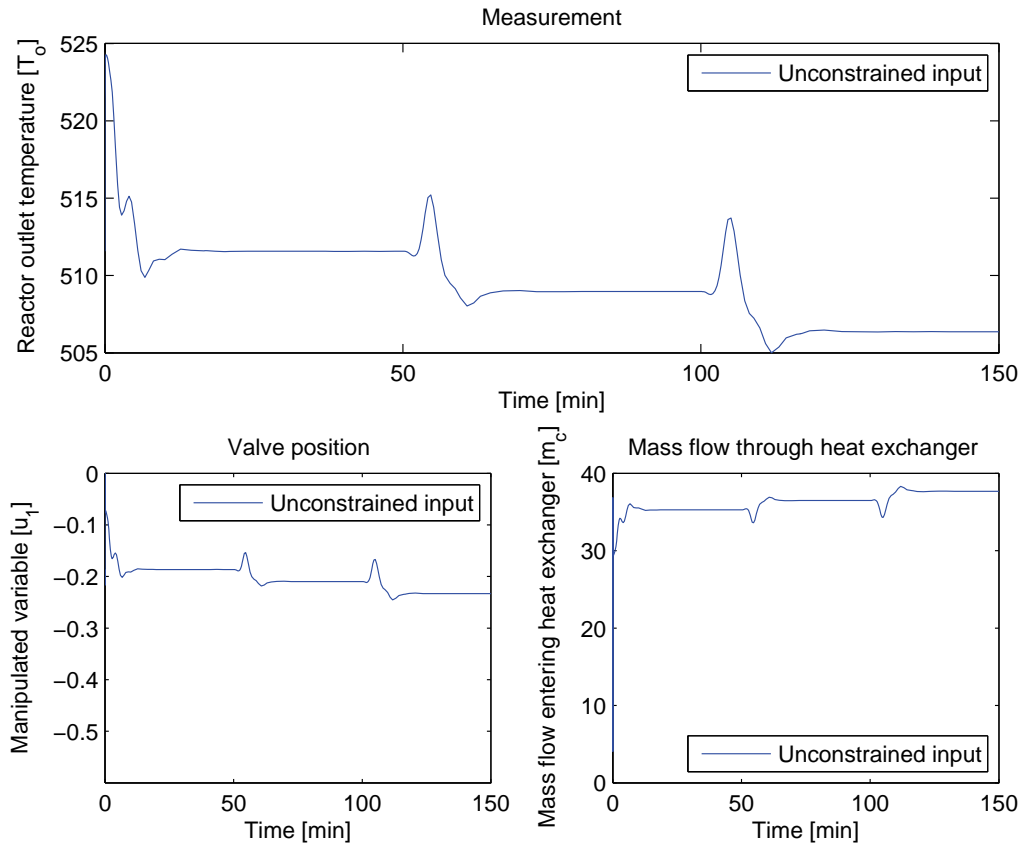


Figure 5.3: Nonlinear simulation with unconstrained input and temperature feed (T_{feed}) used as disturbance.

the disturbance (T_{feed} and pressure) enters the reactor in exactly the same way as in Figure 3.1. The figure also shows that the RHP-zeros causes the inverse response.

Morud [Mor96] claimed that the RHP-zeros most likely would not limit the performance of the reactor, which is probably true, based on the simulations in Figure 5.3. Simulations in the subsequent section will show that controlling the reactor in

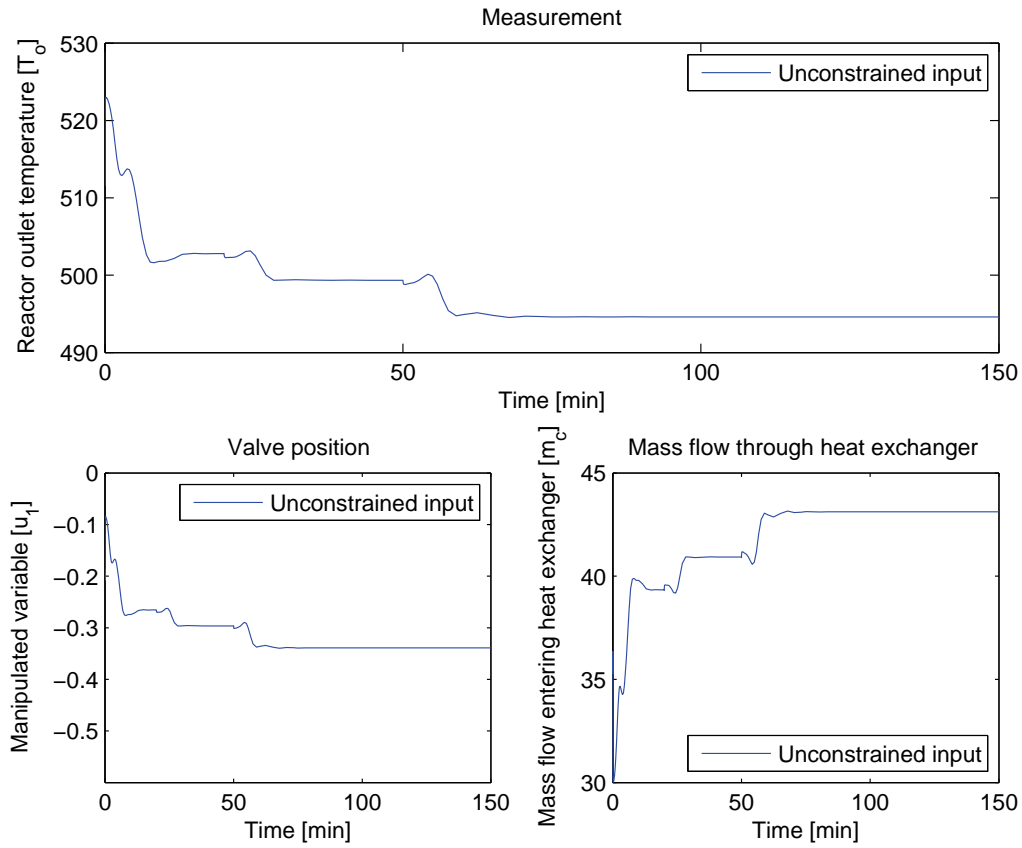


Figure 5.4: Nonlinear simulation with unconstrained input and pressure used as disturbance.)

face of larger disturbances, will be difficult.

5.2.2 Constrained Input

From the industrial data found in Morud[Mor96], one will find that the temperature feed (T_{feed}) mass flow through the first quench (Q_1) is 16.1111 kg/s and that the mass flow entering the heat exchanger (m_c) is equal to 35.2778 kg/s. Based on the provided data and the constraints given in Equation 2.20, i.e.;

$$-0.5 \geq u_1 \leq 0.5 \quad (5.1)$$

it implies that the upper constraint (0.5) refers to the situation where the valve is fully closed, i.e., the mass flow; $m_1 = m_c + Q_1$ bypasses the heat exchanger. The lower constraint will refer to the opposite situation, i.e., all the mass flow entering quench 1, will come from the heat exchanger.

In order to saturate the valve, a greater disturbance than the one given in the previous chapter is necessary. Figure 5.5 shows the performances of the system when a decrease from 250 to 215°C in temperature feed occur. The simulation results are shown both for the unconstrained and constrained case.

The figure shows the simulation for 2 different cases, where the temperature drops

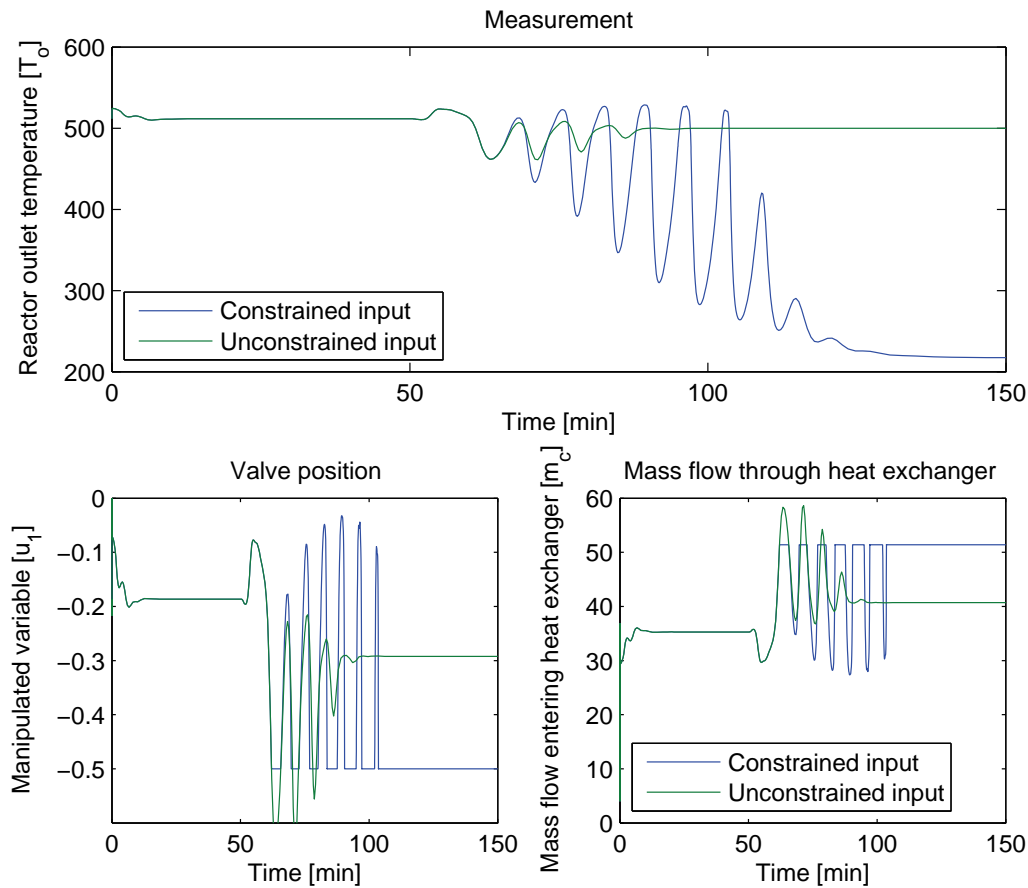


Figure 5.5: Nonlinear simulation with constrained input. The green line shows the unconstrained and the blue line shows the result for the constraint case. The temperature feed is reduced from 250°C to 215°C at $t=50$ min in both simulations.

from 250°C to 215°C in both cases. The first simulation shows the simulation result

for the unconstrained case. It can be seen from the figure that the controller stabilizes the ammonia reactor, but the figure down to the left reveals that the input violates the lower constraint. Thus, a negative mass flow enters quench 1, i.e., a mass flow greater than m_1 is entering the heat exchanger. This situation is obviously unrealistic.

The second simulation shows the case where constraints are added to the input. It can be seen from the figure that the reactor outlet temperature starts to oscillate and after a while, settles at the lower operating point which refers to extinction of the reaction. From the figure down to the left, it can be seen that the manipulated variable saturates at the lower constraint. And thereby tries to compensate by letting less of the mass flow go through the heat exchanger, which is causing the temperature oscillation (and eventually, the extinction).

The simulation results given in Figure 5.5 shows that the RHP-zeros will be a limitation in face of larger disturbances (and with a simple PD-controller). The next section will show that the feedforward strategies will prevent the oscillations from occurring and therefore also the settlement at the lower steady-state operating point. That is, by preventing the manipulated variable from trying to counteract when the saturation occur, it will also prevent the instability.

5.2.3 Feedforward

The ammonia reactor given in this thesis is maybe not the best example to apply the feedforward strategies in question. A thorough discussion of why, is given in Chapter 6. The only way to show a case where the feedforward strategies prevents the oscillations from occurring are given in Figure 5.6. The simulation results are only applicable in a small disturbance range. A larger disturbance will make the reactor temperature oscillate and/or make it settle at the lower (undesired) steady state (reference is made to Chapter 6).

The disturbance model used in the feedforward strategy based on the stable disturbance model is linearized around $T_{\text{feed}}=250^{\circ}\text{C}$ and pressure, $p=200$. The input constraints are equal to the one given in the previous section. The two feedforward strategies based on the unstable disturbance model give exactly the same result. Therefore, only the feedforward based on the "reference governor" approach is shown in the figure.

The figure shows that both feedforward strategies prevents the temperature oscillations and therefore also that the reactor outlet temperature settles at the lower operating point. That is, it prevents the input from starting to counter the oscillations when a decrease in temperature feed (T_{feed}) occurs.

It is difficult to see this from the figure (from the two lower plots), but it is only the feedforward strategy based on the stable disturbance model which counters the inverse response in the beginning of the simulation. The feedforward strategy based on the unstable disturbance (reference governor approach) model does nothing to counter for the inverse response.

The notable in the simulation results is that both strategies settles the manipulated variable at the lowest constraint, even though the controller begins at the initial condition: $u_1=-0.1864867705$, which represents the initial mass flows used in the study of Morud[Mor96] ,i.e., 16.1111 kg/s bypasses and 35.2778 kg/s enters the heat exchanger. The feedback path is broken in the current situation, so stabilization must be preserved by the feedforward alone.

Applying the result of Glover[Glo84] given in Equation 4.1, I found that the minimal achievable bound on KG in this situation is $\|GS\|_{\infty} = 13.4$, which is quite larger than 1. The result is not surprising since the RHP-poles are located close to the imaginary axis, which confirms that the manipulated variable will saturate in response to disturbance.

As already stated, the feedforward strategy is only applicable in a small disturbance range. The reason is that the manipulated variable does not have the sufficient freedom to stabilize the reactor temperature at a too low feed temperature. By influencing the reactor with a greater temperature decrease, will the feedforward strategies still do nothing to counter the disturbance, but this does not help since the reactor

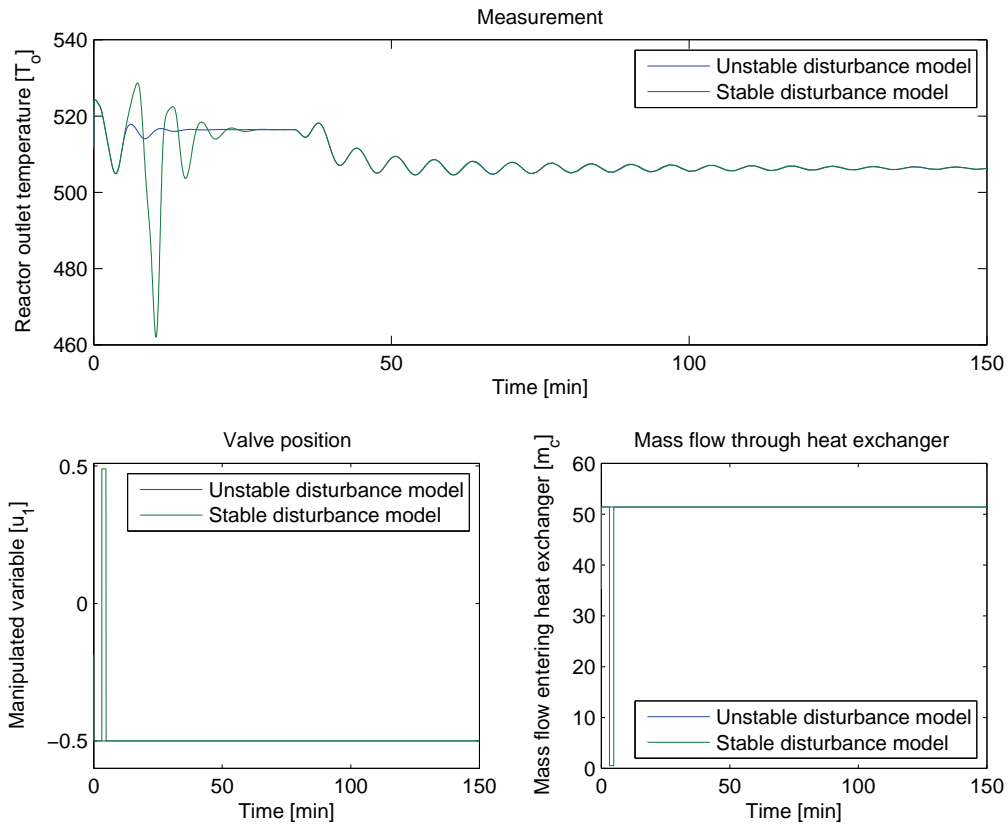


Figure 5.6: Nonlinear simulation with constrained input and feedforward. The blue line represents the output with the feedforward design based on the stable disturbance model. The green line is for design based on the unstable model. At $t=50$, T_{feed} is reduced from 250°C to 215°C .

temperature can not be stabilized by the controller with the given feed temperature.

The simulation results shown are with the temperature feed used as disturbance. There were no pressure disturbances in which similar results were obtained. The main reason is probably that the pressure (as a disturbance) has more influence on the reactor system than the temperature feed. Recall that the temperature feed only mixes with the reactor concentration in the three quench points and in the heat exchanger. The pressure is a part of the chemical reaction in every single discretization point (there is thirty of them in the reactor used in this thesis).

Chapter 6

Discussion

6.1 Reactor Model

All the numerical parameters used in the simulations of the ammonia reactor are taken from the study of Morud[Mor96]. The numerical parameters are given in Appendix A. It is important to keep in mind that these parameters are typical operational parameters and that some of these parameters will change when control is applied to the reactor. The most important one, is the heat exchanger efficiency coefficient (ϵ). There is also important to have in mind that other reactors may operate with different parameters and at different operating conditions.

6.2 Reactor Temperature and Pressure

This thesis is only concerned with the disturbances pressure and temperature feed. An explanation of the effect these parameters have on the reactor may therefore be of interest.

As temperature increases, the amount of ammonia produced decreases since the reaction is exothermic. Reducing the temperature means the system will produce more heat since energy is a product of the reaction. Thus, one might believe that a low temperature is to be used during the reaction. However, the rate of the reaction at lower temperatures is extremely slow, so a higher temperature must be used in order to speed up the reaction which results in a lower amount of produced ammonia. Because of the chemical equilibrium, the temperature for maximum conversion decreases with the increase in ammonia concentration.

Increasing the pressure results in a higher reaction rate and thereby leading to an increase in temperature. The opposite situation is why a decrease in reactor pressure leads to temperature instability.

6.3 Extinction and Instability

In this thesis it is shown that a decrease in fresh feed temperature and pressure can make the reactor unstable. As a result, two different situations may occur. The reactor temperature can start to oscillate or be too low in order to make the conversion possible. These two situations and the damage which could appear as result were treated in Section 3.1

Another important reason to maintain a high temperature is that the effect on toxic waste in the catalysts (e.g., oxygen compounds) may become more severe as the temperature decreases (see, e.g., Fastrup et. al.[B. 10]).

In this thesis, the instability and extinction are equally emphasized. That is, the control of the ammonia reactor is regarded as not satisfactory if the system stabilizes at the lower operating point.

Also note that instability and extinction may depend on other parameters, such as inert amount of the synthesis gas and reaction concentration. The instability may be initiated by one of these parameters, as well as by other conditions in the ammonia synthesis. Remember that in this thesis only the reactor included one heat exchanger is studied. The instability or extinction may as well be caused by changes elsewhere in ammonia synthesis, e.g., in separator or compressor.

Jouny[Juo97] claims that the synthesis reaction rate is very important in order to reproduce the industrial reactors behavior. Because of this claim, it has been important to develop a model, as equal as possible, to those found in Morud[Mor96], Skogestad et.al.[SM98] and Jouny[Juo97].

J. Morud[Mor96] states in his thesis that the instability occurs when the heat exchanger area (A) becomes sufficiently high (reference is made to Equation 2.11). Based on the provided data found in the study of Morud one find that the heat exchanger area (A) is constant. So, I will assume that Morud related the heat transfer area to the heat exchanger efficiency coefficient, ϵ , which is consistent with the findings in this work. An explanation may be of interest.

Consider Equation 2.11 given in Section 2.3:

$$NTU = \frac{UA}{\dot{m}_{cold}C_{cp}} \quad (6.1)$$

The simulations in this assignment are carried out with a constant value of the parameters heat transfer coefficient (U) and heat transfer area (A). The (cold stream) mass flow on the other hand, is increased in order to stabilize the reactor. The result is that the value of number of transfer units (NTU) decreases, which leads to lower heat exchanger efficiency (ϵ), transfer rate (Q) and thereby also lower temperature at the heat exchanger outlet / reactor inlet (see Equation 2.13 and 2.15).

The time did not allow carrying through simulations with higher heat exchanger

area coefficient, A. Maybe the simulation results will look different with higher heat exchanger area included.

6.4 Control of Reactor

The controllers used in this thesis do not eliminate the problem of extinction and they will always make the reactor temperature settle at the lower steady state operating point when the oscillations becomes large. J.Morud [Mor96] proposes to control the reactor in the same manner as given in Section 3.4. That is, using the mass flow through the first quench to control the reactor inlet temperature and cascade a slow controller on the top. This can be done since the first controller loop can be made quite fast as this control loop does not contain any RHP-zeros.

Another possibility can be to implement a more advanced controller in cascade over the controller used in this thesis, e.g., MPC. It would be a slightly "overkill" to use this type of controller on the reactor only, but using it to control the whole ammonia synthesis given in Figure 2.1 would eliminate the problem of extinction. In addition, it would enable the possibility to increase the throughput and optimize the performance of the ammonia synthesis.

J.Morud[Mor96], Morud and Skogestad[SM98] and G. Jouny[Juo97] states in their papers that a PI-controller can stabilize the reactor when the reactor outlet temperature is used as measurement. This applies in most cases, but with this specific reactor model, derivative action must be included in order to stabilize the model. The simulation studies showed that it was not possible to stabilize it with integral action included. The reactor model in question can though be stabilized with a PD-controller.

A P-controller stabilizes the reactor in the case were the reactor inlet temperature is used as measurement. The system will exceed the physical limitations (when constraints are not applied to the input), if one includes integral or derivative action.

Skogestad and Poslethwaite[Mor96] state that with plant models with a zero at the origin, there is only possible to achieve tight control at high frequencies. Thus good transient behaviour is possible, but the control has no effect at steady-state. Based on the linearization in this thesis, one find that one zero is at the origin.

6.5 Feedforward

The ammonia reactor model used in this thesis is perhaps not the best example to apply the feedforward design in question. The reason is (most likely) a combination of; the presence of the (undesired) lower steady-state operating point (corresponds to

extinction of reaction), the positive feedback from the heat exchanger and the range of actuation for the manipulated variable. A physical explanation may be of interest.

The controller stabilizes the reactor by feeding more mass flow through the heat exchanger. The result of feeding more (of the cold stream) mass flow through the heat exchanger, is that less of the mass flow enters the quench without being preheated. This can obviously be done to a limited extent only.

Consider the situation where a decrease in temperature feed from 250°C to 230°C occurs. The position of the valve will settle at $u_1 = -0.4648$ in order to stabilize the reactor in this case, i.e., a mass flow of 49.58 kg/s enters the heat exchanger (only 1.81 kg/s in bypass). A disturbance larger in magnitude (say $T_{\text{feed}} = 210^\circ\text{C}$) will saturate the valve, which will result in temperature oscillations since the mass flow through the heat exchanger is too low in order to stabilize the reactor.

Including the feedforward strategy in this situation will not help, since the manipulated variable is not able to stabilize the reactor at the new operating point. The feedforward element (K_f) does nothing to counter the effect of the disturbance, but that is not enough since the mass flow through the heat exchanger is too small in order to stabilize the reactor with a feed inlet temperature of 215°C. The range of actuation for the manipulated variable is not sufficiently large in order to avoid saturation.

The reactor system will settle at the lower operating point when influenced by larger disturbance. This is also the reason why it is not possible to find an unstable operating point, with eigenvalues (poles) further into the right half plane.

The feedforward strategies were not applicable when pressure was the influencing disturbance. This is not surprising since it was only applicable in a small disturbance range for the case where temperature feed was the influencing disturbance and that pressure as disturbance has more influence on the system than temperature feed.

Someone will maybe find it somewhat strange that the unconstrained and feedforward simulations, for the case where the reactor inlet temperature is used as output, are not given in Chapter 5. From the beginning of the semester, this was the purpose. The reason why it is omitted is simply because it was not possible to find disturbances where the feedforward principles were applicable. An explanation can be that this control loop, which is a simple mixing process with no RHP-zeros included, is quite fast compared to the overall reactor response time of 10 min. This will mean that we can not make use of the slow dynamics inherent by the three beds (reactor).

The conventional feed forward strategy based on Equation 1 is not shown in the simulations given in Chapter 5. It can be shown though, that the system will immediately saturate. The reason for not showing it, was because it difficult to get a representative figure.

6.6 Simulink Model

A lowpass filter was designed in order to avoid algebraic loop problem in Simulink. This was only necessary during the simulations where the reactor inlet temperature (T_i) was used as measurement. The low pass filter was applied after the manipulated variable in the model.

The simulations in this thesis are carried out in Simulink and the solver used during the simulations are Ode 23b (stiff / Tr-BdF2), simply because it was the fastest one. The simulations are carried through with various solvers, all the solvers resulted in the same simulation results.

During the simulations, the upper constraint on the manipulated variable ($u=0.5$), had to be slightly smaller ($u=0.495$). The reason is that zero mass flow through the heat exchanger resulted in a zero in the denominator in Equation 2.15, which resulted in an error in Simulink. However, it is not realistic that this slightly change had any influence on the simulation results obtained.

As a closure to this discussion, a few words about the MATLAB Function block, used to develop the mass and energy balances, should be mentioned. As stated earlier in the discussion, the reactor outlet temperature (output) will stabilize at the lower operating point in the case were large disturbance (in temperature feed) occur. By trying to get the output unstable from the lower operating point, the following error occurs in MATLAB:

Evaluation of expression resulted in an invalid output. Only finite double vector or matrix outputs are supported.

If this warning is created as a result of the mass and energy equations, or that the MATLAB function block is not suitable for this type of modeling, is not known to the author.

If this model is going to be used in other projects, it would probably be a good idea to replace the MATLAB function block with S-functions to see if the error occur as a result of the equations or the MATLAB function block.

Chapter 7

Conclusion

This thesis has presented a Simulink model of an adiabatic fixed bed ammonia synthesis reactor consisting of three beds, with heat integration and with fresh temperature quenching between the beds. The temperature oscillations analyzed by Morud[Mor96] and Skogestad et. al.[SM98] were recreated and different control strategies were applied in order to stabilize and prevent extinction of the ammonia synthesis reactor.

Feedforward is applied to the plant model with the the reactor outlet temperature as measurement (T_o). The feedforward design is based on the description given in the paper; Feedforward for stabilization, written by Morten Hovd and Robert Bitmead[HB07]. The feedforward design is demonstrated for two different cases; with a stable and an unstable disturbance model.

The main conclusions in this work can be summarized by the following items:

1. The simulations showed that controlling the temperature which enters the first bed (T_i), using the mass flow before the first quench as input, stabilizes the ammonia reactor. This proved that stabilization of the ammonia synthesis is not limited by the RHP-zeros.
2. Stabilization of the ammonia reactor is accomplished with the temperature outlet as measurement (T_o) and the RHP-zeros do not present a serious limitation, but if the reactor is influenced by larger disturbances the controller may not be able to stabilize the reactor.
3. The ammonia reactor was not the best case study for the feedforward strategy in question. The reason is a combination of the positive feedback from the heat exchanger, the presence of the lower steady-state operating point and the range of actuation for the manipulated variable.

4. The feedforward strategies were implemented and shown for the case where the reactor outlet temperature were used as measurement, but the feedforward strategies were only applicable in a small disturbance range.
5. The feedforward strategies were not applicable under any circumstances for the case where the reactor inlet temperature was used as measurement or where pressure is the disturbance influencing the reactor system.
6. There is a trade off between making more of the (cold stream) mass flow go through the heat exchanger and making the cold stream mass flow get mixed with the reactor flow between the beds (at the quench points). So, increasing the amount of the (cold stream) mass flow, does not increase the range of input actuation.
7. The pressure as the influencing disturbance has more influence on the reactor than temperature feed (T_{feed}).
8. The Nehari extension used to find a (stable) approximation of an anti-stable (part of a) transfer function gives a poor approximation when the poles are located close to the imaginary axis.
9. An attempt on designing a H_{∞} -controller were carried out. This design was not applicable to the state-space model(s) made. Reformulation of the control problem is necessary in order to apply the H_{∞} -controller.
10. The controller structures and controllers used in this thesis does not exclude the problem with extinction.
11. The system can not be stabilized with a PI-controller. Derivative action must be included in order to stabilize the ammonia reactor when the control loop includes the RHP-zeros.

Chapter 8

Further Work

This chapter of recommended work is divided into two sections since it turned out that the ammonia reactor is not the best study for the feedforward strategies in question. Although, simulations with a higher heat exchanger area should be carried out. Proposals of further work using the ammonia reactor in this thesis are given in the first section. The second section describes in what models the feedforward strategy should be implemented in.

8.1 Control of Ammonia Reactor

The first obvious extension to this assignment is to prevent the occurrence of extinction. One may implement a controller using the method proposed by Morud, with a slow controller on top of the controller which is using the mass flow through the first quench to control the inlet temperature to the first bed.

Another approach could be to apply a more advanced controller to the whole (or larger section of the) ammonia synthesis plant, e.g., MPC. In fact, Mark Cannon et al.[KC01] states that a NMPC should be applied to the ammonia synthesis because of the nonlinear process dynamics and frequent changes in operating points. Skogestad and Postlethwaite[SP07] also states that plants with RHP-zeros can be stabilized using non-causal controllers.

8.2 Feedforward

With regards to the feedforward strategies described in this thesis, the proposal would be to not try to implement it with the given reactor model (reference made to Chapter 8).

If implementing the feedforward strategies are preferred, it should be on a system where the disturbance is not influenced by the strong integration, the tight coupling between manipulated variable and disturbance and without the presence of the lower steady state operating point, which one will find in the reactor used in this assignment.

With the feedforward strategy based on an unstable disturbance model, one should probably find a disturbance model with RHP-poles further into the right half plane if one will use the Nehari extension used in this thesis.

It may be an idea to try to apply the H_∞ -controller, but a reformulation of the state-space models is then necessary. I am afraid that the H_∞ -controller may behave in the same manner as the result given in this thesis.

Appendix A

Numerical Parameters used in the Simulations

All the numerical parameters used in the simulations of the ammonia reactor are taken from the study of Morud[Mor96]. The reaction is stoichiometric and the reaction synthesis and the equations used in the simulation were given in section 2.2.2. The steady-state temperature profile is found by Newton-Raphson iteration (see Appendix C). There exists three steady-states, where we mainly are interested in the upper one.

Numerical parameters:

Gas heat capacity, C_{pg}	3500 J/kg,K
Heat capacity, C_{pc}	1100 J/kg,K
Heat of reaction $-\Delta H_{rx}$	$2.7 \cdot 10^6$
Volume, bed 1	$6.69 m^3$
Volume, bed 2	$9.63 m^3$
Volume, bed 3	$15.2 m^3$
Catalyst bulk density	$2200 kg/m^3$
Typical gas density	$50 kg/m^3$
Dispersion coefficient bed 1, Γ_1	$5.6 \cdot 10^{-4}$
Dispersion coefficient bed 2, Γ_1	$5.6 \cdot 10^{-4}$
Dispersion coefficient bed 3, Γ_1	$5.6 \cdot 10^{-4}$
Number of discretization points in each bed	10

Typical operating conditions:

Inlet flow through preheater, m_c	127 tons/h
Flow out of reactor, m_h	252 tons/h
Quench bed 1, Q_1	58 tons/h
Quench bed 2, Q_2	35 tons/h
Quench bed 3, Q_3	32 tons/h
Inlet mole fraction, NH_3	0.0417
Feed mole fraction, N_2	0.2396
Feed mole fraction, H_2	0.7187
Feed gas temperature, T_{feed}	250°C
Reactor pressure, p	200 bar

Heat exchanger parameters:

Heat transfer coefficient, U	536 W/m^2K
Heat exchanger area, A	283 m^2
Calculated number of heat transfer units, NTU	1.23
Calculated heat exchanger efficiency	0.629

Appendix B

Numerical Solution of the Model Equations

The model equations (Equation 2.1 and 2.2) may be solved as follows.

The reactor beds are discretized with grid spacing Δz . The energy balance given by Equation 2.2 has the following form:

$$\frac{\partial T}{\partial t} + \frac{\partial T}{\partial z} = K \cdot r(T, c) + \frac{\partial^2 T}{\partial z^2} \quad (\text{B.1})$$

By Taylor series expansion to second order, the following finite difference approximations for the space derivatives are obtained:

$$\frac{T_j - T_{j-1}}{\Delta z} = \frac{\partial T}{\partial z} - \frac{\Delta z}{2} \frac{\partial^2 T}{\partial z^2} + O(\Delta z^2) \quad (\text{B.2})$$

$$\frac{T_{j+1} - 2T_j + T_{j-1}}{\Delta z^2} = \frac{z}{2} \frac{\partial^2 T}{\partial z^2} + O(\Delta z^2) \quad (\text{B.3})$$

Introducing these into Equation B.1 yields:

$$\frac{\partial T_j}{\partial t} = K \cdot r(t, c) - u \frac{T_j - T_{j-1}}{\Delta z} + \left(\Gamma - \frac{u\Delta z}{2}\right) \frac{T_{j+1} - 2T_j + T_{j-1}}{\Delta z^2} \quad (\text{B.4})$$

Consider next the mass balance given by Equation 2.1, which can be seen to have the following form:

$$\frac{\partial c}{\partial t} + u_w \frac{\partial c}{\partial z} = \frac{C_p}{C_{pc}} r(T, c) \quad (\text{B.5})$$

This equation can be solved in the same manner. Then the following discretized equations for mass and energy in cell number i are obtained:

$$\frac{\partial c_i}{\partial t} = c(i-1) - c(i) + \frac{dm_k r(T, c)}{\dot{m}_k} \quad (\text{B.6})$$

$$\frac{\partial T_i}{\partial t} = \frac{(\dot{m}_k C_p (T(i-1) - T(i)) + dm_k r(T, c))}{dm_k C_{pc}} \quad (\text{B.7})$$

where dm_k is the mass of catalyst and \dot{m} is the mass flow in each bed. The subscript k refers to the k 'th bed ($k=1,2$ or 3). The subscript i , refers to the discretization segment (ten in each bed). Where the relation:

$$u_w = \frac{\dot{m}_k C_{pg}}{m_{cat} C_{pc}} \quad (\text{B.8})$$

has been used and where m_{cat} is the catalyst mass in each bed [kg].

The ammonia system is now reduced to a system of ordinary differential equations for temperatures T_i and concentration c_i , and may be integrated in time using any numerical method.

Appendix C

MATLAB Files

The MATLAB and Simulink files are handed over together with the thesis. The MATLAB files are still given below for clarity.

C.1 MATLAB Functions used in each Bed

```
function [ybed1]=bed1(Tin1,cf,p,T,c,m1)
%-----Parameters-----
Cp=3500;          % gas
Cpc=1100;         % catalyst
Nbed1=10;        % No. of discretization points; 10 in each bed
rhoc=2200;
vol1=6.69;
dHrx=2.7e6; % [kJ/kg] Note: 111370 * 28 = 3.118 e6
dm1=vol1/Nbed1*rhoc; % mass of catalyst in each bed
%-----
% Conc. in bed 1:
dcdt(1)=cf-c(1)+dm1*rx(p,T(1),cf)/m1;
for i=2:10
    dcdt(i)=c(i-1)-c(i)+dm1*rx(p,T(i),c(i-1))/m1;
end
%-----temperature-----
%Dtdt in bed 1:
dTdt(1)=(m1*Cp*(Tin1-T(1))+dm1*rx(p,T(1),cf)*dHrx)/(dm1*Cpc);
for i=2:10
    dTdt(i)=(m1*Cp*(T(i-1)-T(i))+dm1*rx(p,T(i),c(i-1))*dHrx)/(dm1*Cpc);
```

```

end
ybed1=[dTdt dcdt];

function [ybed2]=bed2(Tin2,cin2,p,T,c,m2)
%-----Parameters-----
Cp=3500;           % gas
Cpc=1100;          % catalyst
Nbed2=10;          % No. of discretization points; 10 in each bed
rhoc=2200;
vol2=9.63;
dHrx=2.7e6; % [kJ/kg] Note: 111370 * 28 = 3.118 e6
dm2=vol2/Nbed2*rhoc; % mass of catalyst in each bed
%-----
% Concentration in bed 2
dcdt(1)=cin2-c(1)+dm2*rx(p,T(1),cin2)/m2;
for i=2:10
    dcdt(i)=c(i-1)-c(i)+dm2*rx(p,T(i),c(i-1))/m2;
end
% Temperature in bed 2
dTdt(1)=(m2*Cp*(Tin2-T(1))+dm2*rx(p,T(1),cin2)*dHrx)/(dm2*Cpc);
for i=2:10
    dTdt(i)=(m2*Cp*(T(i-1)-T(i))+dm2*rx(p,T(i),c(i-1))*dHrx)/(dm2*Cpc);
end
ybed2=[dTdt dcdt];

function [ybed3]=bed3(Tin3,cin3,p,T,c,m3)
%-----Parameters-----
Cp=3500;           % gas
Cpc=1100;          % catalyst
Nbed3=10;          % No. of discretization points; 10 in each bed
rhoc=2200;
vol3=15.2;
dHrx=2.7e6; % [kJ/kg] Note: 111370 * 28 = 3.118 e6
dm3=vol3/Nbed3*rhoc; % mass of catalyst in bed 3
%-----
% Concentration in bed 3
dcdt(1)=cin3-c(1)+dm3*rx(p,T(1),cin3)/m3;
for i=2:10
    dcdt(i)=c(i-1)-c(i)+dm3*rx(p,T(i),c(i-1))/m3;
end
end

```

```

%----- Temperature -----
dTdt(1)=(m3*Cp*(Tin3-T(1))+dm3*rx(p,T(1),cin3)*dHrx)/(dm3*Cpc);
for i=2:10
    dTdt(i)=(m3*Cp*(T(i-1)-T(i))+dm3*rx(p,T(i),c(i-1))*dHrx)/(dm3*Cpc);
end
ybed3=[dTdt dcdt];

```

C.1.1 Reaction Rate

```

function r=rx(p,T,c)
% r - reaction rate [kg NH3/ kg cat, s]
% T - temperature [C]
% c - mass fraction NH3 [-]
% Assumes noe inert and stoichiometric mixtures of N2 and H2

mNH3=c; % mass fraction ammonia
mH2=(1-c)*6/34;
mN2=(1-c)*28/34;
nNH3=mNH3/17;
nH2=mH2/2;
nN2=mN2/28;
x=nNH3/(nNH3+nH2+nN2)*1; % mole fraction ammonia

R=8.31;
k1=1.79e+4*exp(-87090/(R*(T+273)));
k2=2.57e+16*exp(-198464/(R*(T+273)));
pnh3=x*p ; % partial pressure (bar)
pn=(1-x)*0.25*p;
ph=(1-x)*0.75*p;
r=k1*pn*ph^1.5/pnh3 - k2*pnh3/ph^1.5; % [mol N2/ m3 cat, h]
r=r*34/2200/3600; % [kg NH3/ kg cat, s]
r=4.75*r;% Multiply by 4.75 to match industrial instability

```

C.2 State-space Models

```

global mc mh Cp Cpc Q1 Q2 Q3 Npoint Tfeed cf dm1 dm2 dm3 dHrx u conc p c
c=0.08*ones(1,30);
mc=127*1000/3600; % flow entering heat exchanger (kg/s)

```

```

mh=252*1000/3600; % total feed flow (kg/s)
Cp=3500;          % gas
Cpc=1100;         % catalyst
Q1=58*1000/3600; % quench flows (kg/s)
Q2=35*1000/3600;
Q3=32*1000/3600;
Npoint=30;        % No. of discretization points; 10 in each bed
cf=0.08; % feed mass fraction of ammonia
rhoc=2200;
vol1=6.69;
vol2=9.63;
vol3=15.2;
dHrx=2.7e6; % [kJ/kg] Note: 111370 * 28 = 3.118 e6
dm1=vol1/Npoint*3*rhoc; % mass of catalyst in each bed
dm2=vol2/Npoint*3*rhoc;
dm3=vol3/Npoint*3*rhoc;
fcorr=0.5; epsnr=1.e-4; % decrease fcorr if convergense problems
p = 200;          % Reactor pressure, bar
Tfeed=224;        % Fresh feed temperature, C
% -----

```

```

%-----
%                               Steady-state
%-----
%Taken from Morud(1997), Tinit determines which steady state you will find
%Tinit=linspace(340,460,30); % should give middle steady-state; To=437.31
Tinit=linspace(360,510,30); % should give upper steady-state; To=511.565
Tss=ssnr(Tinit,fcorr,epsnr);
Tinit10=Tinit(1:10);
Tinit20=Tinit(11:20);
Tinit30=Tinit(21:30);
delta=0.001;
% A-matrix with c(i)=c(i-1)+.....
for i=1:Npoint
    perturb=zeros(Npoint,1);
    perturb(i)=delta;
    pert1 = righthand(0,Tss+perturb')';
    pert2 = righthand(0,Tss-perturb')';
    A(:,i)=( pert1 - pert2 )/(2*delta);
end

```

```

end
%-----Eigenvalues-----
%Tfeed=250 (constant)
%Tfeed[crit]=232
% p=170: Barely unstable with eigenvalues 0.0002+- 0.0148i
%           where 1/0.0148 = 67.5 sec
%           Limit of instability is at about 172 bar.
% p=200: Stable; eigenvalues furthest to right -0.0017+- 0.0183i
% p=165: Unstable with eigenvalues 0.0007 +- 0.0143i where

%-----
% p=200 (constant)
% p[crit]=172 bar
% Tfeed=250:   Stable; eigenvalues furthest to right -0.0017 +- 0.0183i
% Tfeed=240:   Stable; eigenvalues furthest to right -0.0006 +- 0.0167i
% Tfeed=230:   Barely unstable with eigenvalues 0.0010 +- 0.0142i
%-----
% B-,C- and D-matrices
u=heatx(Tinit(Npoint),Tfeed);
u0=u;
u=u0-delta; delT1=righthopen(Tinit);
u=u0+delta; delT2=righthopen(Tinit);
u=u0;
B=(delT2-delT1)/(2*delta); B(2:Npoint)=0*B(2:Npoint);
C=zeros(1,Npoint); C(Npoint)=1;
%only the reactor outlet temperature is available for measurement
D=[0];
d=[0 0];
%-----
%                               G(s)
%-----
[num,den]=ss2tf(A,B,C,D);
G=tf(num,den);
zs=zero(G);
ps=pole(G)
[z1,p1,k1]=tf2zp(num,den);
[G_s,G_us]=stabsep(G);
%-----
%                               Disturbance model
%-----

```

```

Bd_p=200*ones(30,1); Bd_p(1)=0; Bd_p(10)=10;Bd_p(20)=0;
Bd_Tf=zeros(30,1);Bd_Tf(1)=250;Bd_Tf(10)=250;Bd_Tf(20)=250;
Bd=[Bd_p Bd_Tf];
Dsys=ss(A,Bd,C,d);
Gd=tf(Dsys);set(Gd,'InputName',{'Pressure','Tfeed'},'Outputname','To');
zd=zero(Gd);
pd=pole(Gd)
%-----
%                               Splitted disturbance model Gd
% Gd_s is the stable part of Gd
% And Gd_us is the unstable part...
% Gd_s is allways strictly proper
%-----
[Gd_s,Gd_us]=stabsep(Gd);
zd_us=zero(Gd_us);
pd_us=pole(Gd_us);
%s=tf('s');
%-----
%                               Gd_us mirrored into the LHP
%-----
% Disturbance transfer function from input "pressure" to output To
% [z1,p1,k1]=zpkdata(Gd_us(1));
% p_temp1=p1{1};
% z_temp1=z1{1};
% pm1=uminus(p_temp1);
% zm1=uminus(z_temp1);
% Gdm1=zpk(zm1,pm1,k1);
% pdm1=pole(Gdm1)
% zdm1=zero(Gdm1)
% pu1=pole(Gd_us(1))
% zu1=zero(Gd_us(1))
% Disturbance transfer function from input "Tfeed" to output To
% [z2,p2,k2]=zpkdata(Gd_us(2));
% p_temp2=p2{1};
% z_temp2=z2{1};
% pm2=uminus(p_temp2);
% zm2=uminus(z_temp2);
% Gdm2=zpk(zm2,pm2,k2);
% pdm2=pole(Gdm2)
% zdm2=zero(Gdm2)

```

```

% pu2=pole(Gd_us(2))
% zu2=zero(Gd_us(2))
% Always control the pole of Gdm, which is the mirrored image of Gd_us...
% The zeros and poles of Gdm and Gd_us should be equal, but with
% opposite sign ,i.e., the poles and zeros of Gdm should be in the LHP, when
% the poles and zeros of Gd_us is in the RHP. Otherwise both is zero.
%-----

```

C.3 Nehari Extension

```

%-----
%Nehari extension
% Made by professor Morten Hovd
Gd_uss = ss(Gd_us);
%Merk: Glovers formler for Nehari extension dekker bare kvadratiske
%systemer.Må derfor tilpasse de to elementene i Gd_uss hver for seg
%ui=1 eller ui = 2)

ui = 2;
[a,b,c,d]=ssdata(Gd_uss);

b = b(:,ui);
d = d(:,ui);

%----- Tilpass koden ovenfor for evt. andre systemer

%Gds = ss(-a,-b,c,d);
Gds = ss(-a',-c',b',d');%'Mirror image of unstable part': ikke bare
% er tiden reversert, men i tillegg må innganger og
% utganger 'byttes om', dvs. man 'sender
% utgangssignalet tilbake til inngangen'.

[Gdsb,g]=balreal(Gds);%Poler nær imaginær akse gir svært stor Hankel
%singulærverdi, og derfor dårlig tilnærming.
[A,B,C,D]=ssdata(Gdsb);

nx = size(A,1);

```

```

I = eye(nx);
P = fliplr(I);

%Reverser rekkefølgen på tilstandene.
Ap = P*A*P';
Bp = P*B;
Cp = C*P';
Dp = D;
Gp = ss(Ap,Bp,Cp,Dp);

%Finn controllability grammian og observability grammian
P = gram(Gp,'c');
Q = gram(Gp,'o');

sig = P(nx,nx);

S1 = P(1:nx-1,1:nx-1);
S2 = Q(1:nx-1,1:nx-1);

Gam = S1*S2-eye(nx-1)*sig^2;
U = -1;
%Eneste mulige valg for SISO systemer(?),
%se (6.23) hos Glover for det generelle tilfellet.

A11 = Ap(1:nx-1,1:nx-1);
B1 = Bp(1:nx-1,:);
C1 = Cp(:,1:nx-1);

Ah = (Gam)\(sig^2*A11'+S2*A11*S1-sig*C1'*U*B1');
Bh = (Gam)\(S2*B1+sig*C1'*U);
Ch = C1*S1+sig*U*B1';
Dh = Dp -sig*U;

Gd_usN = ss(-Ah',-Ch',Bh',Dh')
[Ac,Bc,Cc,Dc]=ssdata(Gd_usN);
[Gdm_num,Gdm_den]=ss2tf(Ac,Bc,Cc,Dc);
Gdm_usN=tf(Gdm_num,Gdm_den)

```


C.4 H_∞ -controller

```
% s=tf('s');
% Gd=(-10*s+1)/((s-1)*(0.2*s+1)*(10*s+1));
% G=5/((10*s+1)*(s-1));
[num,den]=ss2tf(A1,B,C,D);
[dnum,dden]=ss2tf(A1,Bd,C,[0 0],2);
% [num,den]=tfdata(G);
% [dnum,dden]=tfdata(Gd);
G=nd2sys(num,den);
Gd=nd2sys(dnum,dden);

Gtot=sbs(Gd,G);
[Gta,Gtb,Gtc,Gtd]=unpck(Gtot);
[Gta,Gtb,Gtc,Gtd]=minreal(Gta,Gtb,Gtc,Gtd);
Gtot=pck(Gta,Gtb,Gtc,Gtd);
% TwoDOFbound=GAM;
% Gtotb=sbs(Gtot,[1e-4 0]);
Wn=0.00001%0.00001;
systemnames='Gtot Wn';
inputvar=' [n(1);d(1);u(1)]';
outputvar=' [u;d;-Gtot-Wn]';
input_to_Gtot=' [d;u]';
input_to_Wn=' [n]';
sysoutname='P';
cleanupysic='yes';
sysic;

[K,CL,GAM,info]=hinfsyn(P,2,1,0.1,200,1e-4)

TwoDOFbound=GAM

Gtotb=madd(Gtot,[1e-4 0])
systemnames='Gtotb';
inputvar=' [d(1);u(1)]';
outputvar=' [u;-Gtotb]';
input_to_Gtotb=' [d;u]';
sysoutname='P';
cleanupysic='yes';
```

```
sysic
```

```
[K,CL,GAM,info]=hinfosyn(P,1,1,0.1,200,1e-4)
```

C.5 Miscellaneous Functions

```
function Tprime=righthand(t,T)
global mc mh Cp Cpc Q1 Q2 Q3 Npoint Tfeed cf dm1 dm2 dm3 dHrx u conc
% comment: For simplicity we use rx((T(i),c(i-1)))
%rather than rx((T(i),c(i)))

%Mass flows:
m1=mc+Q1;
m2=m1+Q2;
m3=m2+Q3;
% Conc. in bed 1:
%-----
c(1)=cf+dm1*reaxion(T(1),cf)/m1;
for i=2:10
    c(i)=c(i-1)+dm1*reaxion(T(i),c(i-1))/m1;
end
% Quench 2:
%-----
cin2=m1/m2*c(10)+Q2/m2*cf;
% Conc. in bed 2
%-----
c(11)=cin2+dm2*reaxion(T(11),cin2)/m2;
for i=12:20
    c(i)=c(i-1)+dm2*reaxion(T(i),c(i-1))/m2;
end
% Quench 3:
%-----
cin3=m2/m3*c(20)+Q3/m3*cf;
% Conc. in bed 3
%-----
c(21)=cin3+dm3*reaxion(T(21),cin3)/m3;
for i=22:30
    c(i)=c(i-1)+dm3*reaxion(T(i),c(i-1))/m3;
end
```

```

% Quench 1:
%-----
Ti=heatx(T(30),Tfeed); Tin1=mc/m1*Ti+Q1/m1*Tfeed;
% dTdt in bed 1:
%-----
dTdt(1)=(m1*Cp*(Tin1-T(1))+dm1*reaxion(T(1),cf)*dHrx)/(dm1*Cpc);
for i=2:10
    dTdt(i)=(m1*Cp*(T(i-1)-T(i))+dm1*reaxion(T(i),c(i-1))*dHrx)/(dm1*Cpc);
end
% Quench 2:
%-----
Tin2=m1/m2*T(10)+Q2/m2*Tfeed;
% dTdt in bed 2:
%-----
dTdt(11)=(m2*Cp*(Tin2-T(11))+dm2*reaxion(T(11),cin2)*dHrx)/(dm2*Cpc);
for i=12:20
    dTdt(i)=(m2*Cp*(T(i-1)-T(i))+dm2*reaxion(T(i),c(i-1))*dHrx)/(dm2*Cpc);
end
% Quench 3:
%-----
Tin3=m2/m3*T(20)+Q3/m3*Tfeed;
% dTdt in bed 3:
%-----
dTdt(21)=(m3*Cp*(Tin3-T(21))+dm3*reaxion(T(21),cin3)*dHrx)/(dm3*Cpc);
for i=22:30
    dTdt(i)=(m3*Cp*(T(i-1)-T(i))+dm3*reaxion(T(i),c(i-1))*dHrx)/(dm3*Cpc);
end
Tprime=dTdt;
Tin=heatx(T(Npoint),Tfeed);
conc=c;
%-----

function Tss = ssnr(Tinit,fcrr,epsnr)
% Newton-Raphson iteration to find steady-state temperature profile
% of reactor with preheater. (It may be unstable if we do not apply control)
% Tinit - initial temperaure profile
% fcrr - correction for NR-iteration; reduce if convergense problems
% Tss = steady-state temperature profile
global mc mh Cp Cpc Q1 Q2 Q3 Npoint Tf cf dm1 dm2 dm3 dHrx u conc

```

```

% Linearize to find Jacobi matrix
delta=0.001;
for i=1:Npoint
    perturb=zeros(Npoint,1);
    perturb(i)=delta;
    pert1 = righthand(0,Tinit+perturb)';
    pert2 = righthand(0,Tinit-perturb)';
    A0(:,i)=( pert1 - pert2 )/(2*delta);
end
J=inv(A0);

% Newton-Raphson iteration
error=1;
Tss=Tinit;
while error>epsnr
    func=righthand(0,Tss);
    Tss=(Tss'-fcorr*J*func)';
    error=norm(func);
    error_steady_state_temperature_profile=error
end

```

Bibliography

- [B.10] B. Fastrup and H. Nygaard Nielsen. On the influence of oxygen on iron catalysts during ammonia synthesis and catalyst characterization. <http://www.springerlink.com/content/q535826q5680874n/>, Accessed: May 2010.
- [GK90] G.F.Froment and K.B.Bischoff. *Chemical Reactor Analysis and design*. Wiley, 1990.
- [Glo84] Keith Glover. All optimal hankel-norm approximations of linear multivariable systems and their l_∞ -error bounds. Technical report, Cambridge, 1984.
- [Glo86] Keith Glover. Robust stabilization of linear multivariable systems: relations to approximation. Technical report, Cambridge, 1986.
- [HB07] Morten Hovd and Robert R. Bitmead. Feedforward for stabilization. Technical report, Engineering Cybernetics Norwegian University of Science and Technology and Department of Mechanical and Aerospace Engineering of California San Diego, 2007.
- [JGBF03] Trond Andersen Jens G. Balchen and Bjarne A. Foss. *Reguleringsteknikk*. NTNU-trykk, 2003.
- [Juo97] Gintas Juonys. Msc thesis; stability of ammonia and methanol reactors, 1997.
- [Kar04] Vinay Kariwala. *Doctor of philosophy: Multi-loop controller synthesis and performance analysis*. PhD thesis, University of Alberta, 2004.
- [KB86] Frank Kreith and Mark S. Bohn. *Principles of Heat Transfer*. Thomson learning, 1986.
- [KC01] Basil Kouvaritakis and Mark Cannon. *Nonlinear predictive control: theory and practice*. The Institution of Electrical Engineers, 2001.

- [KZG96] John C. Boyle Kemin Zhou and Keith Glover. *Robust and Optimal Control*. Prentice Hall, 1996.
- [Mor96] John Morud. *Dr. Ing. thesis; Studies on the dynamics and operation of integrated plants*. PhD thesis, Chemical Engineering, Norwegian University of Science and Technology, 1996.
- [Pat10] Patrick Gniffke. Ammonia synthesis and production. <http://iir-de.wikidot.com/ammonia-production>, Accessed: May 2010.
- [Sko03] Sigurd Skogestad. Simple analytic rules for model reduction and pid controller tuning. Technical report, Norwegian University of Science and Technology, 2003.
- [SM98] Sigurd Skogestad and John Morud. Analysis of instability in an industrial ammonia reactor. Technical report, Chemical Engineering, Norwegian University of Science and Technology, 1998.
- [SP07] Sigurd Skogestad and Ian Postlethwaite. *Multivariable Feedback Control*. Wiley, 2007.